

PC1-1

Peak Effect Induced by Heavy-ion Irradiation in 2H-NbSe₂ Single Crystals

*Wenjie LI¹, Sunseng PYON¹, Ataru ICHINOSE², Satoru OKAYASU³, Tsuyoshi TAMEGAI¹

Department of Applied Physics, The University of Tokyo¹

Grid Innovation Research Laboratory, Central Research Institute of Electric Power Industry²

Advanced Science Research Center, Japan Atomic Energy Agency³

As an effective method for improving the critical current density (J_c) of superconductors, heavy-ion irradiation is widely used [1]. Columnar defects (CDs) are introduced by heavy-ion irradiations, which are strong pinning centers to suppress vortex motion thus to enhance J_c . Other than J_c enhancement, an anomalous peak effect at $\sim 1/3B_\Phi$ (B_Φ is the dose equivalent matching field, and $B_\Phi = 1$ T corresponds to 5×10^{10} cm⁻² CDs.) was observed in a twinned YBa₂Cu₃O_{7- δ} single crystal when the magnetic field was applied parallel to CDs ($\theta_H = \theta_{CD}$; θ_H and θ_{CD} are angles from the c -axis to the applied field and CDs, respectively.) [2]. In their experiments [2], for distinguishing the effect of CDs introduced by heavy-ion irradiation from that of twin boundaries parallel to the c -axis on J_c , they intentionally introduced tilted CDs ($\theta_{CD} = 30^\circ$). If we can find a superconductor with no correlated defects, the peak effect can be observed without tilting CDs. The conventional low-temperature superconductor NbSe₂ is such a good candidate. Contrary to our expectation, however, the peak effect was not observed when CDs were introduced parallel to the c -axis ($\theta_{CD} = 0^\circ$) and the field was applied along the c -axis ($\theta_H = 0^\circ$) as shown in Fig. 1(a). Although vortex structures for the two cases ($\theta_H = \theta_{CD} = 30^\circ$ and $\theta_H = \theta_{CD} = 0^\circ$) are expected to be very similar intuitively, the results are very different. On the other hand, we have reported the presence of peak effect in NbSe₂ with splayed CDs, where the splay angle is as small as $\pm 5^\circ$ [3]. In the present study, we introduced splayed CDs in NbSe₂ with $\theta_{CD} = \pm 1^\circ$ and observed a similar peak effect by applying magnetic field parallel to the c -axis ($\theta_H = 0^\circ$) as shown in Fig. 1(b). The fact that only $\pm 1^\circ$ splay of CDs induced behavior different from the case of $\theta_{CD} = 0^\circ$ is unexpected. To find possible explanation for the difference between these two cases, studies on the θ_H dependence of J_c are necessary. In order to measure θ_H dependence of J_c efficiently and precisely, we modified the horizontal rotator for SQUID magnetometer (MPMS5-XL) and used small Hall probes set on the rotator to detect the local magnetic field from the sample and external field. We will present the θ_H dependence of J_c on samples with CDs parallel to the c -axis and with splayed CDs ($\theta_{CD} = \pm 1^\circ$), and discuss possible mechanism of the peak effect.

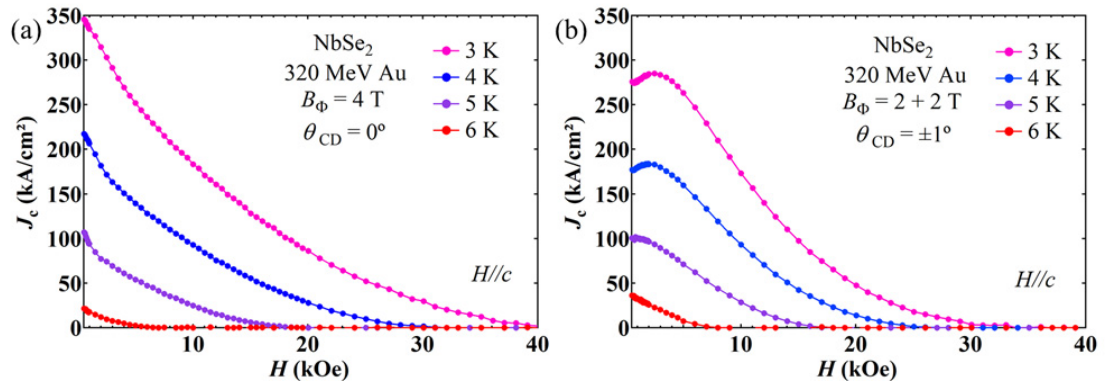
[1] T. Tamegai *et al.*, Supercond. Sci. Technol. 25, 084008 (2012).

[2] L. Civale *et al.*, Phys. Rev. Lett. 67, 648 (1991).

[3] W. Li *et al.*, J. Phys. Conf. Ser. 2323, 012017 (2022).

Fig. 1. Magnetic field dependence of J_c for 2H - NbSe₂ single crystals irradiated by 320 MeV Au (a) along the c -axis ($B_\Phi = 4$ T, $\theta_{CD} = 0^\circ$) and (b) from two directions symmetrically (Total $B_\Phi = 4$ T, $\theta_{CD} = \pm 1^\circ$).

Keywords: NbSe₂, heavy-ion irradiation, peak effect



PC1-2

Turbulent Structures and Characterizations of "11-type" Iron-based Superconductors by Magneto-optical Imaging

*Tong REN¹, Sunseng PYON¹, Tsuyoshi Tamegai¹

Department of Applied Physics, The University of Tokyo¹

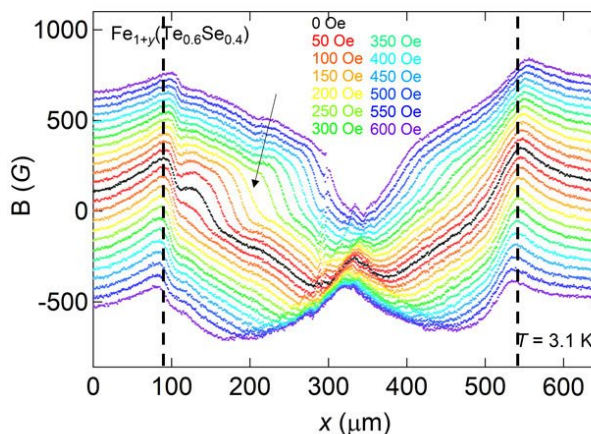
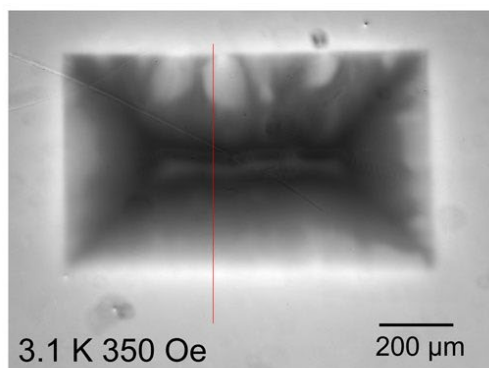
In our preceding study, a turbulent vortex structure at the remagnetization boundary of a superconductor, called the Meissner hole, was reported in a single crystalline '122-type' iron-based superconductor (IBS) $(\text{Ba}_{0.67}\text{Rb}_{0.33})\text{Fe}_2\text{As}_2$ [1]. The Meissner hole was observed in a pristine crystal and the one with artificial defects, accompanied by an excess local current at the remagnetization boundary.

The Meissner hole, we trust, should be a ubiquitous vortex phenomenon that is not bound to one or few dedicated types of superconductors. Recently we observed Meissner hole-like vortex behavior (see attached figure) in the '11-type' IBS $\text{Fe}(\text{Te}_{0.6}\text{Se}_{0.4})$. This material is currently under intense investigation for its potential to realize a topological non-trivial surface state, where the Majorana Fermion is assumed to be hosted. Taking this opportunity, we decide to extend the same magneto-optical observation to its parent material, FeSe. Unlike other iron-pnictide parent compounds like LaFeAsO or BaFe_2As_2 , FeSe undergoes a structural transition at ~ 90 K without being accompanied by antiferromagnetism. The magnetic transition, however, is seemingly cooperative with its superconductivity since it emerges along with the superconducting transition temperature under pressures [2]. More knowledge of this mysterious phase transition requires the resolution of the vortex state below T_c (~ 8 K), which is easily covered by our low-temperature limit for observation (3 K).

[1] T. Ren, S. Pyon, and T. Tamegai, J. Phys. Conf. Ser. 1975, 012013 (2021).

[2] T. Terashima et al., J. Phys. Soc. Jpn. 84, 063701 (2015).

Keywords: Vortex, Magneto-optical imaging, Meissner hole



PC1-3

Observation of vortex clusters using magneto-optical imaging sensors fabricated by an eclipse-PLD method

*Shuuichi Ooi¹, Minoru Tachiki¹, Takashi Mochiku¹, Hayato Ito^{2,3}, Akihiro Kikuchi¹, Shunichi Arisawa¹, Takayuki Kubo^{2,3}, Kensei Umemori^{2,3}

National Institute for Materials Science¹

High Energy Accelerator Research Organization²

SOKENDAI (The Graduate University for Advanced Studies)³

Niobium is a low- κ superconductor with GL parameters close to $1/\sqrt{2}$, the critical value separating type-I and type-II. In high-purity niobium, the vortex-vortex interaction becomes attractive in the intermediate range where the inter-vortex distance is several times the magnetic field penetration length λ , so that a so-called intermediate mixed state appears where the vortex lattice phase with aggregated vortices and the vortex-free Meissner phase are separated [1]. When high-purity niobium is cooled in a low magnetic field less than 100 Oe, vortex clusters are formed due to the attractive interaction. In view of its application to superconducting accelerating (SRF) cavities fabricated with high-purity niobium, contribution of the remanent vortices during cooling is one of the factors limiting the Q-value at sufficiently low temperatures. Therefore, understanding the morphology and dynamics of vortex clusters is helpful to effectively expel vortices from the SRF cavities.

In order to investigate how the clusters form depending on the magnetic field, in present study, we performed magneto-optical imaging observations using $(\text{Bi,Lu})_3(\text{Fe,Ga})_5\text{O}_{12}$ garnet films fabricated by an Eclipse-PLD (pulsed laser deposition) method. As a result, we found that the cluster size decreased monotonically with decreasing magnetic field. This tendency was also confirmed by molecular dynamics simulations assuming a theoretically predicted vortex-vortex interaction.

[1] S. Ooi et al., "Observation of intermediate mixed state in high-purity cavity-grade Nb by magneto-optical imaging", Phys. Rev. B 104, 064504 (2021).

Keywords: Vortex cluster, Niobium, Magneto-optical imaging, Pulsed laser deposition

Simulation of Collective Motion of Vortices Using Molecular + Field Dynamics Method

*Jun Yamanaka¹, Masaru Kato²Department of Physics and Electronics, Osaka Prefecture University¹Department of Physics and Electronics, Osaka Metropolitan University²

In a type II superconductor under an external magnetic field, quantized vortices appear. Controlling vortices is important for application of superconductors. Especially, pinning and dynamics of vortices in a dirty superconductor have been studied widely.

Uchiyama et al investigated collective motion of vortices in a type II superconductor using the scanning tunneling microscope[1]. They found that vortex lattice are divided into vortex bundle separated by the glide plane of edge dislocation. In order to investigate origins of this collective motion of vortices, we simulate vortex dynamics in a moderately dirty superconductor using the molecular dynamics method (MD).

The MD is a computer simulation method for many particle dynamics, in which we solve equations of motion of particles numerically. In order to apply this method to the vortex dynamics, we treat vortices as particles in two dimensional space. The equation of motion for i -th vortex is given as,

$$\eta(dr_i)/dt = f_{di} + f_{pi} + f_{vi} + f_{fi}$$

where η is a viscous drag coefficient, r_i is an position of i -th vortex, f_{di} is a driving force by an external current, f_{pi} is a pinning force, f_{vi} is a interaction force between vortices and f_{fi} is a thermal fluctuation force. Here, we neglect an inertia term, because this term is relatively small comparing with the viscous term. The vortex interaction force f_{vi} comes from all remaining vortices. This make the calculation time become large and the number of vortices that can be treated is only a few hundreds. Because the vortex interaction comes from the current around other vortices, the interaction between vortices can be treated as the Lorentz force from the current field. Also, the external current can be included into the current field.

In the extended molecular dynamics equation of motion for i -th vortex is given as,

$$\eta(dr_i)/dt = f_{ci} + f_{pi} + f_{fi}$$

where is f_{ci} is force by the current field. Pinning force f_{pi} is given as,

$$f_{pi} = -\nabla V_{imp}(r) |_{(r=r_i)}$$

and thermal fluctuation force f_{fi} is given as,

$$\langle f_{fi}(t_1) \cdot f_{fj}(t_2) \rangle = 2\eta k_B T \delta_{ij} \delta(t_1 - t_2).$$

The Lorentz force f_{ci} from the current field is derived from the overall total current J consisting of vortex currents and the external current is given as,

$$f_{ci} = (1/c) J(r_i) \times \Phi_0 z.$$

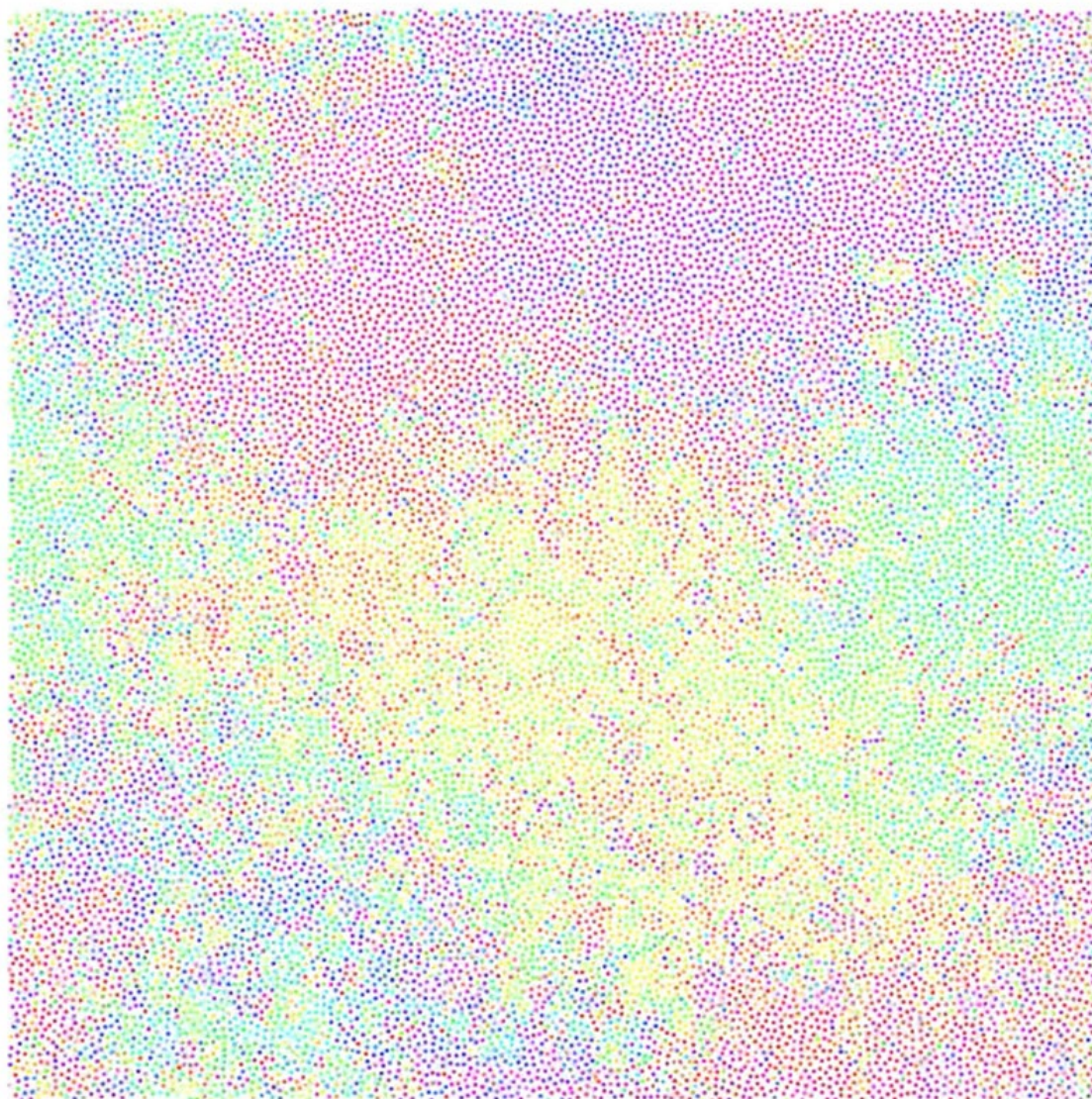
We consider $50 \lambda_0 \times 50 \lambda_0$ a square superconducting plate. In order to obtain the impurity potential and the current field, we use the finite element method (FEM). In the FEM, we divide the superconducting plate into random triangular elements. The maximum value of the impurity potential is V_{impmax} . We show simulation results of the dynamics of the 20000 vortices as shown in Figure.

[1]K. Uchiyama, S. Suzuki, A. Kuwahara, K. Yamasaki, S. Kaneko, H. Takeya, K. Hirata, N. Nishida; Physica

C, 470 (2010) S795.

Keywords: Molecular Dynamics Method, Vortex Dynamics, Collective Motion, Vortex Pinning

{t =, 0.41, vortex number = , 20 000}



Vortex states under in a superconductor under a helical magnetic field

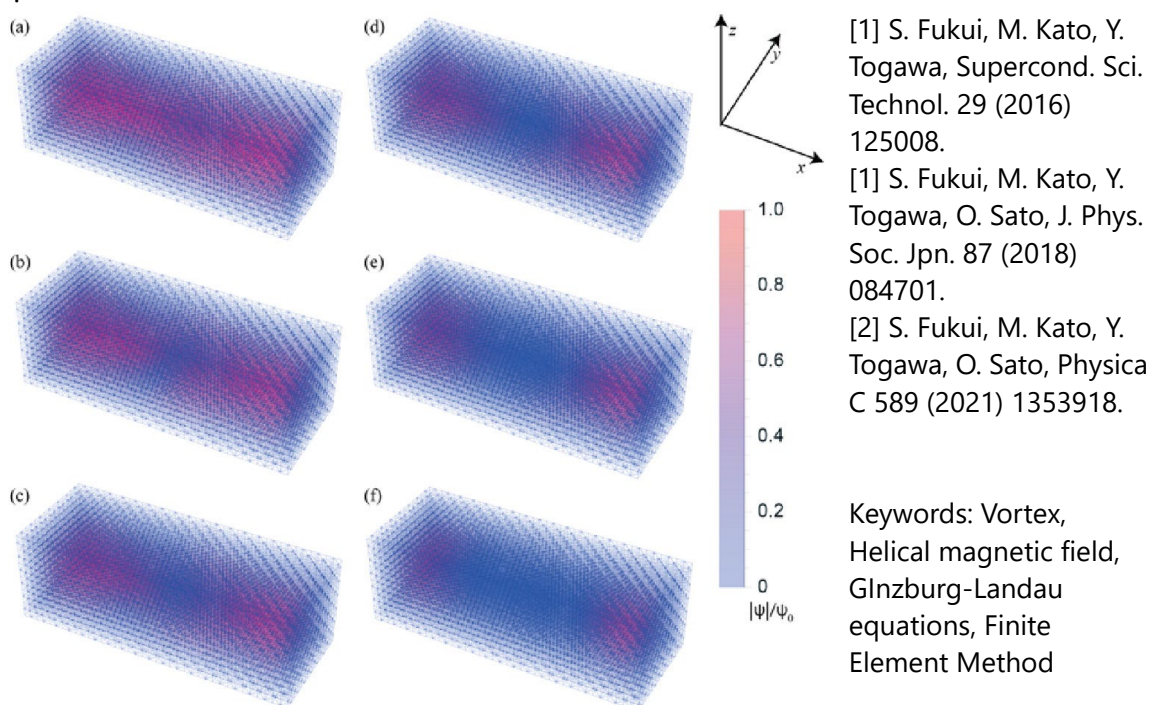
*Masaru Kato¹Osaka Metropolitan University, Japan¹

Under an external field in a superconductor, there appear vortices. In a usual situation, the magnetic field is aligned in a single direction. So, all of vortices are parallel to the magnetic field. However, if the magnetic field is rotated, e.g. a double layer structure with a superconductor and a helical magnet, vortices might be rotated. When several vortices appear, these vortices interact with each other. The interaction between parallel vortices has been studied well. But the interaction between rotated vortices has not been studied well until now.

Previously, we studied vortex structure in a superconductor under a helical magnetic field. Solving the 3-dimensional Ginzburg-Landau (GL) equations with the 3-dimensional finite element method (3d-FEM), we obtained unusual magnetic structure (Fig.1) [1-3]. In Fig. 1, directions of two vortices are not parallel to those of the magnetic field.

In order to investigate vortex structures in detail, we consider several helical magnetic fields and solve the 3-d GL equations with the FEM. We find that superconducting transition temperature depends on the rotation pitch of the helical magnetic field. Also, vortex-vortex interaction depends on an angle between vortices. Sometime, they form an entangled structure. Moreover, cutting and reconnection of vortices occur. We will investigate the origin of these unusual vortex behaviors.

Figure.1 vortex structures under a helical magnetic field.



Effect of thermal fluctuation on voltage state in an intrinsic Josephson junction

*Takamasa Wachi¹, Masaru Kato²Osaka Prefecture University Japan¹Osaka Metropolitan University Japan²

When a current applied to an intrinsic Josephson junction (IJJ) in a copper oxide high-temperature superconductor is increased, the IJJ enters a voltage state and then the voltage increases stepwise. After these voltage states, when the current is lowered, THz oscillation occurs. The voltage state is described as a running state of a particle in a washboard potential, using the RCSJ model of the Josephson junction (JJ).

In this study, solving coupled layered JJ model with thermal fluctuation current and using the finite element method (FEM). We investigate these voltage state in the IJJ. [1]

We consider an IJJ model with seven JJ layers. Fig. 1 shows time evolution of the spatial average $\langle\varphi\rangle$ of the phase difference $\Delta\varphi(dt)$. Fig. 1 (a), (b), (c), (d) and (e) shows time evolutions of the spatial average of the phase difference for $j_{ext}/j_c = 1.0, 2.0, 5.0, 10.0$ and 13.0 respectively. Here, j_c is a critical current of the JJ. In Fig. 1, blue line, orange line, green line and red line show time evolutions of the spatial average of the phase difference in the first, second, third and fourth JJ layer, respectively.

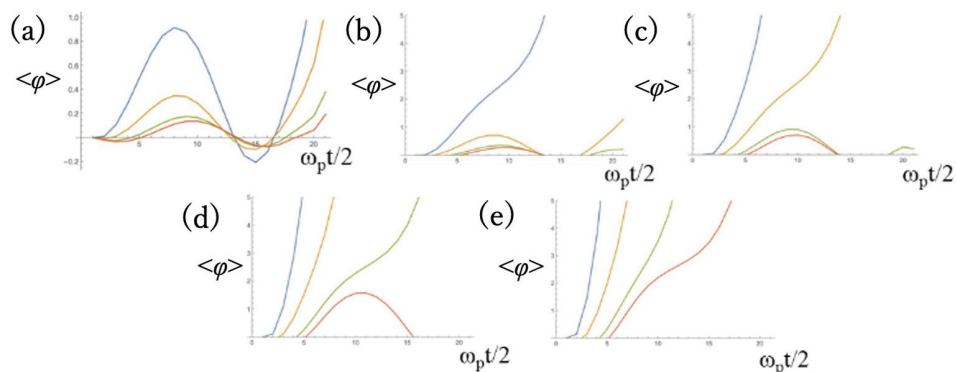
In Fig. 1 (a), the first JJ becomes voltage state first. Then, second JJ becomes voltage state due to the coupling between first and second JJ's (Fig. 1 (b)). Also, we found that when the coupling between layers becomes strong switch to the voltage state easily, the inner JJs and the effect of thermal fluctuation current becomes smaller.

We will also report the results of simulations in which the thermal fluctuation force is applied to the phase.

Figure 1. The time evolution of the spatial average of phase differences in the first, second third and fourth JJ layer at $j_{ext}/j_c = 1.0$ (a), $j_{ext}/j_c = 2.0$ (b), $j_{ext}/j_c = 5.0$ (c), $j_{ext}/j_c = 10.0$ (d) and $j_{ext}/j_c = 13.0$ (e).

[1]. T. Wachi and M. Kato, to be published in J. Phys. Conf. Ser.

Keywords: intrinsic Josephson junction, finite element method, switching to voltage state



PC2-1-INV

High Temperature Spin-Triplet Superconductivity in $K_2Cr_3As_3$

*Guo-qing Zheng¹

Department of Physics, Okayama University¹

Spin-triplet superconductivity is a rare quantum phenomenon and is particularly fascinating from the topological perspective, as such novel superconductors can host Majorana bound states that can be used in topological quantum computing. Although spin-triplet state has long been sought, concrete evidence had been lacking until 2016 when $Cu_xBi_2Se_3$ with a critical temperature $T_c \sim 3.5$ K was unambiguously proved to be in such state [1]. Recently, $A_2Cr_3As_3$ ($A = Na, K, Rb, Cs$) superconductors with T_c as high as 8 K have emerged as a new class of materials with ferromagnetic spin correlations [2, 3]. In this presentation, we show in $K_2Cr_3As_3$ single crystal ($T_c = 6.5$ K) that, the spin susceptibility measured by ^{75}As Knight shift remains unchanged across T_c with the magnetic field applied in the ab plane, but is reduced in the superconducting state when the field is along the c axis, vanishing toward zero temperature [4]. Such spontaneous emergence of spin nematicity unambiguously indicates that $K_2Cr_3As_3$ is a spin-triplet superconductor described by a vector order parameter d that is parallel to the c axis. We further find that the interaction dictating the d -vector direction is less than 13 T. We discuss the multiple-phases feature of the superconducting state, and show that $K_2Cr_3As_3$ is a new platform for the study of topological superconductivity at the highest temperature ever.

References

- [1] K. Matano, M. Kriener, K. Segawa, Y. Ando, G.-q. Zheng, Nature Physics 12, 852 (2016).
- [2] J. Yang et al., Phys. Rev. Lett. 114, 147002 (2015).
- [3] J. Luo et al., Phys. Rev. Lett. 123 047001 (2019).
- [4] J. Yang, J. Luo, C. Yi, Y. Shi, Y. Zhou, and G.-q. Zheng, Sci. Adv. 7, eabl4432 (2021).

PC2-2-INV

Multiple superconducting phases and field-induced superconductivity in UTe₂ with spin-triplet state

*Dai Aoki¹

IMR, Tohoku University¹

UTe₂ attracts much attention because of spin-triplet superconductivity and unusual properties[1]. It crystallizes in the body-centered orthorhombic structure with the space group, Immm (#71). The large Sommerfeld coefficient ($\gamma=120$ mJ K⁻²mol⁻¹) manifests a heavy electronic state. Superconductivity occurs at 1.5-2K in the paramagnetic ground state. One of the highlights in UTe₂ is the huge upper critical field, H_{c2} , exceeding the Pauli limit. In particular, the field-reentrant superconductivity appears up to the first-order metamagnetic transition at $H_m=35$ T. Thus the spin-triplet state is naively expected. Microscopic evidence for the spin-triplet state is indeed obtained from the Knight shift in NMR experiments. At the moment of the discovery of superconductivity, UTe₂ had been thought to be at the verge of ferromagnetic order with strong ferromagnetic fluctuations from the similarity to the ferromagnetic superconductors, URhGe and UCoGe, where the field-reentrant (-reinforced) superconductivity is observed when the field is applied along the hard magnetization axis, leading to the development of ferromagnetic fluctuations. In UTe₂, ferromagnetic fluctuations are, however, not confirmed experimentally, alternatively, antiferromagnetic fluctuations with the incommensurate q-vector are detected in the inelastic neutron scattering experiments. In UTe₂, multiple fluctuations antiferromagnetic/ferromagnetic fluctuations as well as valence, and Fermi surface instabilities may play important roles for superconductivity. Another important highlight in UTe₂ is the multiple superconducting phases under pressure and the field-induced phenomena, which also support a spin-triplet scenario because of the spin and orbital degree of freedom. In this talk, we present our recent progress on UTe₂, focusing on the high quality single crystal growth and superconducting properties.

[1] See review paper, for example, D. Aoki, J. P. Brison, J. Flouquet, K. Ishida, G. Knebel, Y. Tokunaga, Y. Yanase, J. Phys.: Condens. Matter. 34, 243002 (2022).

PC2-3-INV

Nonreciprocal electric responses in superconductors

*Youichi Yanase¹, Akito Daido¹, Hikaru Watanabe², Hiroto Tanaka¹, Yuhei Ikeda¹

Department of Physics, Kyoto University (Japan)¹

Research Center for Advanced Science and Technology, University of Tokyo (Japan)²

We show the theoretical framework of various nonreciprocal responses in superconductors. The superconducting diode effect, nonlinear superconducting optics, and nonreciprocal Meissner effect are discussed, and observation in noncentrosymmetric superconductors and parity-breaking superconductors is proposed.

First, stimulated by the recent discovery of the superconducting diode effect (SDE) [1], we propose an intrinsic mechanism to cause the SDE [2]. The SDE refers to the nonreciprocity of the critical current. We show that the SDE is caused by the nonreciprocity of the Landau critical momentum and propose that the crossover phenomenon in the helical superconducting state can be proved by the SDE. The intrinsic SDE unveils the rich phase diagram and functionalities of noncentrosymmetric superconductors.

Second, we show that superconductors with the space-inversion symmetry breaking host giant nonreciprocal optical responses, such as the photocurrent generation and second harmonic generation [3]. Divergent behaviors are attributed to the nonreciprocal superfluid density and the Berry curvature derivative, characteristic of parity-breaking superconductors. These indicators quantify the performance of superconductors in nonlinear optics. We also show the microscopic conditions for the nonreciprocal optical responses in noncentrosymmetric superconductors [4].

The nonreciprocal correction to the superfluid density also leads to the nonreciprocal Meissner effect, namely, asymmetric screening of magnetic fields due to the nonreciprocal magnetic penetration depth. Performing a microscopic analysis of an exotic superconductor UTe_2 , we show that the nonreciprocal Meissner effect is useful for probing parity-mixing properties and gap structures in superconductors [5].

[1] F. Ando, Y. Miyasaka, T. Li, J. Ishizuka, T. Arakawa, Y. Shiota, T. Moriyama, Y. Yanase, and T. Ono, *Nature* 584, 373 (2020).

[2] Akito Daido, Yuhei Ikeda, Youichi Yanase, *Phys. Rev. Lett.* 128, 037001 (2022).

[3] Hikaru Watanabe, Akito Daido, Youichi Yanase, *Phys. Rev. B* 105, 024308 (2022).

[4] Hiroto Tanaka, Hikaru Watanabe, Youichi Yanase, arXiv:2205.14445.

[5] Hikaru Watanabe, Akito Daido, Youichi Yanase, *Phys. Rev. B* 105, L100504 (2022).

Keywords: Nonreciprocal responses, Noncentrosymmetric superconductors, Parity-breaking superconductors, Superconducting diode effect

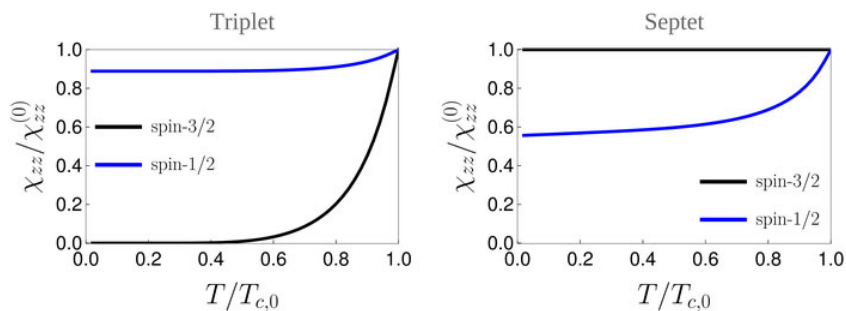
Magnetic response of superconductors with strong spin-orbit coupling

David C. Cavanagh¹, Daniel F. Agterberg², *Philip M. Brydon³Department of Physics, University of Otago, New Zealand¹Department of Physics, University of Wisconsin-Milwaukee, USA²Department of Physics and MacDiarmid Institute for Advanced Materials and Nanotechnology, University of Otago, New Zealand³

A key experimental probe of the pairing symmetry of unconventional superconductors is the pair-breaking effect of an external magnetic field. However, many materials of current interest have multiple bands crossing the Fermi energy and possess strong spin-orbit coupling, which renders the usual single-band theory invalid. In particular, the spin-orbit coupling in a multiband system can lead to anisotropic Zeeman-splitting and introduce gap nodes. In this work we develop a general theory for the pair-breaking effect of an arbitrary external perturbation in such a system. Our central result is that the pair-breaking can be quantified by a single measure which we dub the "field-fitness function", which incorporates the interplay spin-orbital texture of the normal-state bands with both the pairing potential and the perturbation. This parameter controls the suppression of the critical temperature and, for the case of an external magnetic field, the magnitude of the Knight shift in the superconducting state. For even-parity superconductors we find that the field-fitness function for an external magnetic field is one, implying maximal pair-breaking consistent with Anderson's theorem. For odd-parity superconductors, in contrast, the field-fitness function reveals a more complicated interplay which can yield counter-intuitive behaviour. We apply our method to the topical case of p -wave pairing in the effective $j=3/2$ electronic states of the Luttinger-Kohn model. Focusing on the triplet and septet states, we find that the response to a magnetic field depends sensitively on whether the $j=3/2$ or $j=1/2$ band crosses the Fermi energy. In the former case, we find that the septet state is completely insensitive to the Zeeman splitting, whereas this is maximally pair-breaking for the triplet state. Our work offers a convenient tool to understand the magnetic response of many unconventional superconductors. Ref: D. C. Cavanagh, D. F. Agterberg, and P. M. R. Brydon, arXiv:2207.01191 (2022).

Caption: Spin-susceptibility in the p -wave triplet (A_{1u}) and septet (A_{2u}) states of the Luttinger-Kohn model with both $j=1/2$ and $j=3/2$ Fermi surfaces.

Keywords: odd-parity superconductivity, spin-orbit coupling, magnetic field



PC2-5

Unconventional pairing states from fluctuating order: Role of superconducting fitness

*Yufei Zhu¹, Philip.M.R Brydon¹

University of Otago¹

We study unconventional pairing mediated by nearly critical fluctuations of a non-superconducting order parameter that involves multiple degrees of freedom. This is motivated by the observation that superconductivity often appears close to other ordered states in experimental phase diagrams. We propose a general theory in the weak coupling regime that qualitatively connects the pairing strength with the compatibility of the pairing states and the fluctuating orders. The key ingredients are the time-reversal symmetry of the order and the superconducting fitness function. We prove our theory is universal for any electron-electron interaction which is sufficiently peaked in momentum space about the ordering vector. Our theory is applied to the spin-1/2 and spin-3/2 systems accounting for the fermiology. We propose that the superconducting fitness function can be used as a guide to identify unconventional pairing instabilities.

Keywords: fluctuating orders, unconventional superconductivity

PC3-1-INV

Enhanced superconductivity and ferroelectric quantum criticality in strontium titanate

*Martin Greven¹

University of Minnesota¹

Plastic deformation is the permanent distortion that occurs when a material is subjected to stresses that exceed the material's yield strength. While plastic deformation has been used by blacksmiths and engineers for thousands of years, its effects on the electronic properties of quantum materials have been largely unexplored. In this talk, I will review our recent [1,2] and ongoing efforts to understand the effects of compressive plastic deformation in complex oxides. I will primarily focus on SrTiO₃, for which we have uncovered enhanced, low-dimensional superconductivity and ferroelectric quantum criticality correlated with the appearance of self-organized dislocation structures, as revealed by diffuse neutron and X-ray scattering [2,3]. These results demonstrate the potential of plastic deformation and dislocation engineering for the manipulation of electronic properties of quantum materials.

Work funded by the US Department of Energy through the University of Minnesota Center for Quantum Materials, under grant number DE-SC-0016371.

[1] D. Pelc *et al.*, Nat. Commun. 10, 2729 (2019);
<https://doi.org/10.1038/s41467-019-10635-w>

[2] S. Hameed, D. Pelc *et al.*, Nat. Mater. 21, 54 (2022);
<https://www.nature.com/articles/s41563-021-01102-3>

[3] See also: M. Li and Y. Wang., Nat. Mater. 21, 3 (2022);
<https://doi.org/10.1038/s41563-021-01146-5>

Keywords: quantum materials, plastic deformation, superconductivity, ferroelectricity

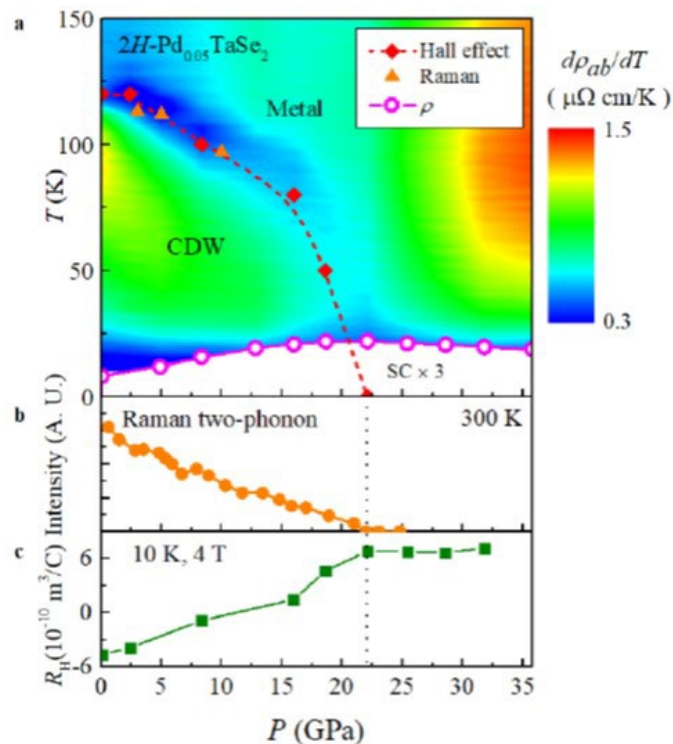
PC3-2-INV

Enhanced superconductivity near a pressure-induced CDW quantum critical point in Pd-intercalated TaSe₂

*Kee H Kim^{1,2}

Department of physics and astronomy, Seoul National University¹
Institute of Applied Physics, Seoul National University²

We present doping and pressure-induced optimization of superconductivity, particularly focusing on tuning of electronic states in Pd-intercalated TaSe₂ i.e. Pd_xTaSe₂, in which superconducting transition is optimized from 0.14 (TaSe₂) to 3.1 K ($x \sim 0.08$) with simultaneous suppression of a commensurate charge density wave (CDW) state. We found that the Pd intercalation can involve a Lifshitz transition in the underlying electronic states at normal states without CDW ground states, which seems to be useful for increasing density of states (DOS) and electron-phonon coupling and in turn two-band BCS superconductivity at low temperatures, albeit its relative importance to enhance superconductivity is not clear yet. Furthermore, an increase of DOS in the vicinity of a doping-induced collapse of a commensurate CDW state can certainly help increase DOS and optimize superconducting transition. Although it was not clear with intercalation, with the tuning of pressure, we found that a second-order quantum phase transition of a CDW transition can occur around 22 GPa, and fluctuating CDW ground states can instigate the superconductivity up to 8.3 K. With systematic Raman and transport results, we discuss how a CDW quantum criticality and related fluctuation can be involved in the process of boosting up superconductivity.



PC3-3-INV

Deep Learning Model for Finding New Superconductors

*Tomohiko Konno¹, Hodaka Kurokawa², Fuyuki Nabeshima², Yuki Sakishita², Ryo Ogawa², Iwao Hosako¹, Atsutaka Maeda²

The National Institute for Information and Communications Technologies¹
The University of Tokyo²

Exploration of new superconductors still relies on the experience and intuition of experts, and is largely a process of experimental trial and error. In one study, only 3% of the candidate materials showed superconductivity [1]. Here, we report the first deep learning model for finding new superconductors. We introduced the method named “reading periodic table” that represented the periodic table in a way that allows deep learning to learn to read the periodic table and to learn the law of elements for the purpose of discovering novel superconductors which are outside the training data. It is recognized that it is difficult for deep learning to predict something outside the training data. Although we used only the chemical composition of materials as information, we obtained an R2 value of 0.92 for predicting Tc for materials in a database of superconductors. We also introduced the method named “garbage-in” to create synthetic data of non-superconductors that do not exist. Non-superconductors are not reported, but the data must be required for deep learning to distinguish between superconductors and non-superconductors. We obtained three remarkable results. The deep learning can predict superconductivity for a material with a precision of 62%, which shows the usefulness of the model; it found the recently discovered superconductor CaBi2 and another one Hf0.5Nb0.2V2Zr0.3, neither of which is in the superconductor database; and it found Fe-based high-temperature superconductors (discovered in 2008) from the training data before 2008. These results open the way for the discovery of new high-temperature superconductor families. The candidate materials list, data, and method are openly available from the link.

Keywords: Deep learning, Material search, Materials informatics

PC3-4

Optimal alloying in hydrides: Reaching room-temperature superconductivity in LaH₁₀

*Tianchun Wang¹, José A. Flores-Livas^{2,3}, Takuya Nomoto⁴, Yanming Ma^{5,6}, Takashi Koretsune⁷, Ryotaro Arita^{3,4}

Department of Applied Physics, The University of Tokyo¹

Dipartimento di Fisica, Università di Roma La Sapienza²

RIKEN Center for Emergent Matter Science³

Research Center for Advanced Science and Technology, The University of Tokyo⁴

State Key Laboratory of Superhard Materials, College of Physics, Jilin University⁵

International Center of Future Science, Jilin University⁶

Department of Physics, Tohoku University⁷

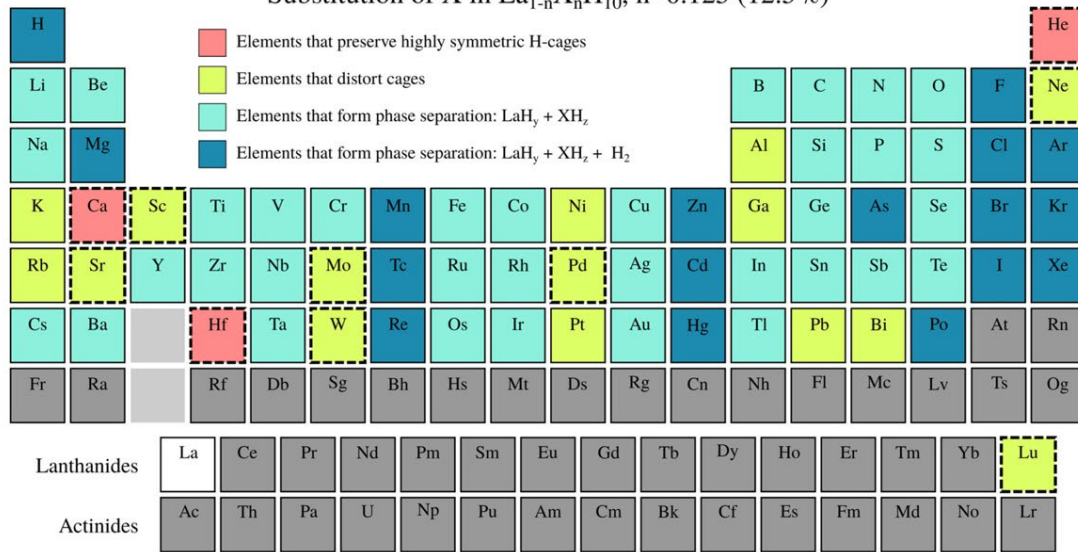
Doping represents one of the most promising avenues for optimizing superconductors, such as reaching record-breaking critical temperatures of hydride superconductors. In this work, we perform a thorough and extensive search for substitutional dopants in LaH₁₀, looking for elements that enhance its electronic structure (especially the density of states at the Fermi level). In total, 70 elements were investigated as possible substitutions of La-sites at the doping ratio of 12.5% under high pressure. By using our systematic and efficient screening protocol, we found Ca as the best candidate dopants, which shift the van Hove singularity and increase the electronic DOS at the Fermi level. With harmonic-level phonon calculations and performing first-principles calculation of T_c , Ca-doped LaH₁₀ shows T_c which is 15% higher than the one of LaH₁₀. It provides a promising route to reach the room-temperature superconductivity in pressurized hydrides by doping.

Fig. 1: Geometry relaxation results of LaH₁₀ doped by different elements with doping ratio of 12.5% at 150 GPa pressure, and different color code gives the behavior for different elements. (a) The periodic table with elements classified to four types of relaxation results. (b) Typical elements with corresponding structural patterns after relaxations for four cases. At the doping ratio of 12.5%, most of the elements destabilized the symmetric pattern, and only 3 elements preserve the high symmetry.

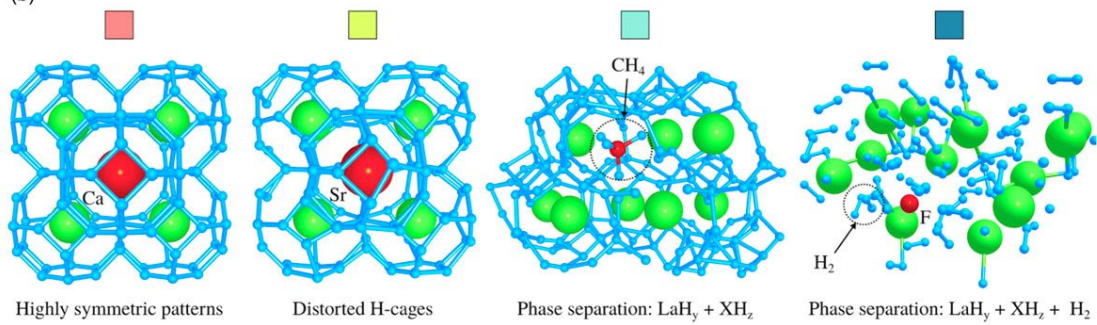
Keywords: Hydride superconductors, Impurities in superconductors, First-principles calculation, van Hove singularity

(a)

Substitution of X in $\text{La}_{1-n}\text{X}_n\text{H}_{10}$, $n=0.125$ (12.5%)



(b)



Bulk electronic structure of layered nitride chloride superconductor Na_xTiNCl studied by HAXPES

Noriyuki Kataoka¹, Masashi Tanaka², Yasumasa Takagi³, Akira Yasui³, Kozo Okada¹, Takanori Wakita¹, Yuji Muraoka¹, Takayoshi Yokoya¹

Graduate School of Natural Science and Technology, Okayama University, Okayama 700-8530, Japan¹

Graduate School of Engineering, Kyushu Institute of Technology, Kitakyushu 804-8550, Japan²

Japan Synchrotron Radiation Research Institute (JASRI)/SPring-8, Sayo, Hyogo 679-5198, Japan³

The layered nitride halides MNX ($M=\text{Ti, Zr, Hf}$; $X=\text{Cl, Br, I}$) have two different polymorphs, α -form and β -form. Both are insulators with a band gap, and when alkali metals are intercalated between the layers, they exhibit superconductivity because of electron doping. The β -form HfNCl is an interesting and well-known superconductor, exhibiting a maximum superconducting transition temperature (T_c) of ~ 26 K[1]. It has been discussed as a candidate for unconventional superconductors based on experimental results, including very small isotope effects due to ^{15}N substitution[2]. On the other hand, TiNCl is known only in the α -form structure and exhibits a T_c of 16 K upon intercalation of alkali metals[3]. Its superconducting properties are different from those of β -form, and the importance of interlayer coupling has been discussed[4]. The possibility that superconductivity is induced by spin and charge fluctuations has also been discussed[5]. Strong electron-electron correlations are often involved in such superconducting mechanisms.

Photoelectron spectroscopy is a powerful tool for studying the electronic structure of strongly correlated systems. However, because it is a surface-sensitive technique and therefore also observes surface electronic states that are different from the bulk electronic states, the bulk electronic states are not always easy to discuss. Therefore, it is important to experimentally investigate the bulk electronic structure of materials such as TiNCl that are sensitive to moist air and oxygen.

In this presentation, we report bulk-sensitive hard X-ray photoelectron spectroscopy (HAXPES) results for the core levels and valence band spectra of Na_xTiNCl ($x=0, 0.1, 0.25, 0.4$). We observe a systematic change in the spectral shape of the core levels and valence band spectra as a function of Na concentration, and find that the electron doping dependence of the Ti 1s spectra is in qualitative agreement with the cluster model calculations. This result suggests that strong correlation effects caused by Ti 3d play an important role for the change in spectral shape.

- [1] S. Yamanaka *et al.*, Nature 392, (1998) 580.
- [2] H. Tou *et al.*, Phys. Rev. B 67, (2003) 100509.
- [3] S. Yamanaka *et al.*, J. Mater. Chem. 19, (2009) 2573.
- [4] S. Zhang *et al.*, Phys. Rev. B 86, (2012) 024516.
- [5] Q. Yin *et al.*, Phys. Rev. B 83, 014509 (2011).

Keywords: Bulk electronic structure, Layered superconductor, strong correlation, HAXPES

PC4-1-INV

Magic-Angle Twisted Graphene Family

*Jeong Min Park¹, Yuan Cao¹, Li-Qiao Xia¹, Shuwen Sun¹, Kenji Watanabe², Takashi Taniguchi², Pablo Jarillo-Herrero¹

Massachusetts Institute of Technology (USA)¹
National Institute for Materials Science (Japan)²

Since the discovery of magic-angle twisted bilayer graphene (MATBG), new moiré systems have been explored to study strongly correlated and topologically nontrivial phenomena. Multiple interesting states, including but not limited to correlated insulators, quantized anomalous Hall states, ferromagnetism, and correlated Chern insulators, have been observed in various moiré materials. However, during the first few years, superconductivity was reproducibly seen only in MATBG. More recently, magic-angle twisted trilayer graphene (MATTG) has shown robust superconductivity and correlated states with an additional knob for electric displacement field tunability. Is it a coincidence? Interestingly, MATBG and MATTG, which are the only robust moiré superconductors known to date, are part of a hierarchy of magic-angle graphene systems, which exhibit a series of twist angles for different number of twisting layers. We experimentally realize magic-angle twisted 4-layer and 5-layer graphene structures, and show that they also exhibit robust superconductivity, therefore establishing alternating-twist magic-angle multilayer graphene as a family of moiré superconductors. With the application of electric displacement and magnetic fields, we find interesting similarities and differences between the members that help us understand the underlying physics behind these systems. In this talk, I will discuss the key data and our current understanding of the magic family, as well as some of our most recent progress.

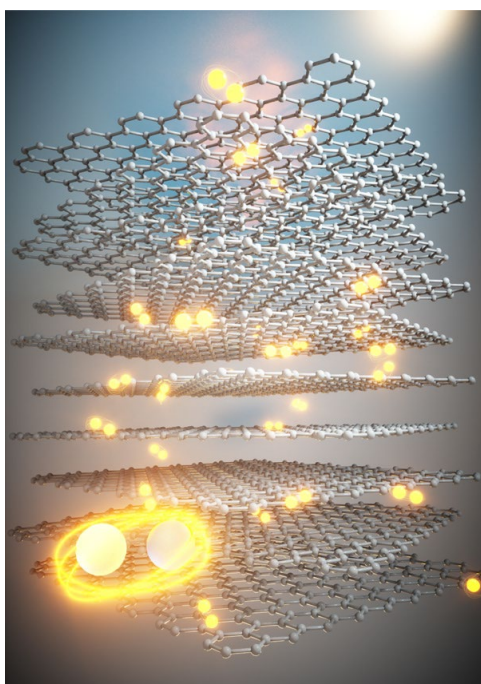


Figure: An artist's illustration of superconducting Cooper pairs in the magic-angle twisted multilayer graphene family

Keywords: Strongly correlated physics, Unconventional superconductivity, Moiré quantum matter, Two-dimensional superlattices

PC4-2-INV

Two-dimensional superconductivity at interfaces and surfaces of KTaO_3

*Yanwu Xie¹

Zhejiang University (China)¹

A new family of oxide-interface superconductors, with a transition temperature (T_c) up to 2.2 K, were recently found at interfaces between KTaO_3 and other oxides (EuO or LaAlO_3) [1-3]. In this talk, we will present our recent progresses in this system. We demonstrate that the superconductivity is sensitive to the orientation of KTaO_3 and find a $T_c \sim 1$ K superconductivity at (110)-orientated interface [2]. We successfully tune the superconducting $\text{LaAlO}_3/\text{KTaO}_3(111)$ interface by applying a gate bias across KTaO_3 [3]. By in-situ transport measurements during growth, we conclude that the formation mechanism of the $\text{LaAlO}_3/\text{KTaO}_3$ interface electron gas is the electron transfer from oxygen vacancies in LaAlO_3 film to KTaO_3 substrate [4]. By exploiting ionic liquid gating, we obtain superconductivity at bare $\text{KTaO}_3(111)$ and (110) surfaces with T_c values up to 2.0 K and 1.0 K, respectively [5], which are almost the same as that in the corresponding interfaces, suggesting that the essential physics of KTaO_3 interface superconductivity lies in the KTaO_3 surfaces doped with electrons.

References

- [1] C. Liu, X. Yan, D. Jin, Y. Ma, H. Hsiao, Y. Lin, T. M. Bretz-Sullivan, X. Zhou, J. Pearson, B. Fisher, J. S. Jiang, W. Han, J.-M. Zuo, J. Wen, D. D. Fong, J. Sun, H. Zhou, and A. Bhattacharya, *Science* 371, 716 (2021) .
- [2] Z. Chen, Z. Liu, Y. Sun, X. Chen, Y. Liu, H. Zhang, H. Li, M. Zhang, S. Hong, T. Ren, C. Zhang, H. Tian, Y. Zhou, J. Sun, and Y. Xie, *Phys. Rev. Lett.* 126, 026802, (2021).
- [3] Z. Chen, Y. Liu, H. Zhang, Z. Liu, H. Tian, Y. Sun, M. Zhang, Y. Zhou, J. Sun, and Y. Xie, *Science* 372, 721,(2021).
- [4] Y. Sun, Y. Liu, S. Hong, Z. Chen, M. Zhang, and Y. Xie, *Phys. Rev. Lett.* 127, 086804, (2021).
- [5] T. Ren, M. Li, X. Sun, L. Ju, Y. Liu, S. Hong, Y. Sun, Q. Tao, Y. Zhou, Z. Xu, and Y. Xie, *Sci. Adv.* 8, eabn4273, (2022).

Keywords: KTaO_3 , interface superconductor, oxide interface , two-dimensional superconductivity

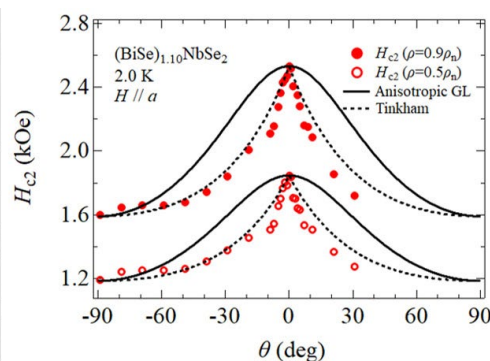
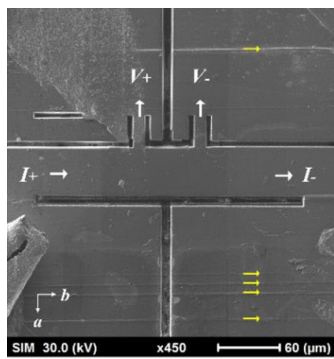
Two-dimensional superconductivity in misfit layered compound $(\text{BiSe})_{1.10}\text{NbSe}_2$ *Soichiro Matsuzawa¹, Haruhisa Kitano², Sunseng Pyon¹, Tsuyoshi Tamegai¹Department of Applied Physics, The University of Tokyo¹Department of Physics, Aoyama Gakuin University²

Misfit layered compounds, denoted by $(MX)_{1+\delta}(TX_2)_n$ ($M = \text{Sn, Pb, Sb, Bi, rare earth metals, T} = \text{Ti, V, Nb, Ta, Cr, X} = \text{S, Se}; n = 1, 2, 3$), are built of alternately double layers MX with quasi NaCl-type structure and TX_2 with slightly distorted trigonal prism [1]. The two sublattices have different spatial symmetry and periodicity from each other, resulting in incommensurability in the in-plane with a misalignment of lattice constants in the a -axis direction. Misfit layered compounds have attracted attention not only for their physical properties such as superconductivity and charge-density wave, but also as materials that can spontaneously realize van der Waals heterostructures.

In this study, we focus on the misfit layered superconductor $(\text{BiSe})_{1.10}\text{NbSe}_2$, which exhibits quasi-two-dimensional behavior. Previously, we have shown that out-of-plane angular dependence of the upper critical field (H_{c2}) of $(\text{BiSe})_{1.10}\text{NbSe}_2$ exhibits a two-dimensional behavior with a cusp fitted by the Tinkham model [2]. On the surface of this material, stripe structures appear along the b -axis direction, *i.e.*, the in-plane alignment direction of the crystal. These stripe structures are unique to many of misfit layered compounds. To investigate the relationship between such a non-uniform crystal structure and the two-dimensional behavior of H_{c2} , we formed a micro-bridge using FIB fabrication to measure uniform regions without stripe structures within a single crystal shown in Fig.1. As a result, we found that the behavior of H_{c2} is still two-dimensional even in sufficiently uniform crystals as shown in Fig.2, indicating that $(\text{BiSe})_{1.10}\text{NbSe}_2$ exhibits an essentially two-dimensional superconducting state. We also investigated the possibility that H_{c2} is enhanced by 3D-2D dimensional crossover or surface superconductivity.

Fig. 1 $(\text{BiSe})_{1.10}\text{NbSe}_2$ single crystal micro-bridge formed by FIB processing.Fig. 2 Out-of-plane angular dependence of upper critical field in $(\text{BiSe})_{1.10}\text{NbSe}_2$ micro-bridge.

[1] G. A. Wieggers, Prog. Solid State Chem. 24, 1 (1996).



[2] S. Matsuzawa, P. Pyon, and T. Tamegai, J. Phys.: Conf. Ser. 2323, 012008 (2022).

Keywords: misfit layered compound, $(\text{BiSe})_{1.10}\text{NbSe}_2$, two-dimensional superconductivity

PC4-4-INV

Superconducting Diode Effect in Rashba Superlattice

*Teruo Ono¹

Kyoto University, Japan¹

The diode effect is fundamental to electronic devices and is widely used in rectifiers and AC-DC converters. However, conventional diodes have an energy loss due to finite resistance. We found the superconducting diode effect (SDE) in Nb/V/Ta superlattices with a polar structure, which is the ultimate diode effect exhibiting a superconducting state in one direction and a normal state in the other [1-3]. SDE can be considered as the nonreciprocity of the critical current for the metal-superconductor transition. We also found the reverse effect, i.e., the nonreciprocal critical magnetic field under the application of the supercurrent [4]. We also found that the polarity of the superconducting diode shows a sign reversal as a magnetic field is increased, which can be considered as the crossover and phase transitions of the finite-momentum pairing states predicted theoretically [5]. SDE in Nb/V/Ta superlattices needs an application of an external magnetic field to break the time reversal symmetry, which is a disadvantage in applications. We recently succeeded in demonstrating SDE in a zero-field by introducing ferromagnetic layers in superlattices. The polarity of the SDE is controlled by the magnetization direction of the ferromagnetic layer, leading to development of novel non-volatile memories and logic circuits with ultralow power consumption.

This work was partly supported by JSPS KAKENHI Grant Numbers (18H04225, 18H01178, 18H05227, 20H05665, 20H05159, 21K18145), the Cooperative Research Project Program of the Research Institute of Electrical Communication, Tohoku University, the Collaborative Research Program of the Institute for Chemical Research, Kyoto University, and the Russian Ministry of Science and Higher Education under Megagrant No. 075-15-2021-607.

References

- [1] F. Ando *et al.*, *J. Magn. Soc. Japan* 43, 17 (2019).
- [2] F. Ando *et al.*, *Nature* 584, 373 (2020).
- [3] F. Ando *et al.*, *Jpn. J. Appl. Phys.* 60, 060902 (2021).
- [4] Y. Miyasaka *et al.*, *Appl. Phys. Express* 14, 073003 (2021).
- [5] A. Daido *et al.*, *Phys. Rev. Lett.* 128, 037001 (2022)

Keywords: Superconducting Diode Effect, Rashba Superlattice

PC4-5

Nonlinear optical responses in two-dimensional superconductors

*Hiroto Tanaka¹, Hikaru Watanabe², Youichi Yanase¹

Department of Physics, Kyoto University, Japan¹

Research Center for Advanced Science and Technology, University of Tokyo, Japan²

A wide variety of optical measurements are key tools for various properties of materials. Especially, nonlinear optics is one of the central fields in physics and has been attracting much attention from fundamental science to technology. For instance, one can apply the second-order nonlinear optical responses to the identification of the phase of exotic matters. It has been demonstrated by measuring the second-harmonic light and direct current generations under the irradiating light [1]. On the other hand, optical responses manifest richer physical consequences such as kinetic inductance in superconductors due to the Cooper pairs' quantum condensation. This may imply synergy between nonlinear optics and superconducting science, namely, superconducting nonlinear optics.

Superconducting nonlinear optical responses may lead to various applications. Owing to the dissipationless property, superconductors may realize efficient interconversions between current and lights. In addition, the responses are expected to be a useful tool for probing the symmetry violations in complex ordered states such as parity symmetry breaking. In light of these interests, a theory of the second-order nonlinear response in superconductors was recently formulated, and a specific Bogoliubov-de Gennes Hamiltonian with a sublattice degree of freedom was investigated numerically [2]. On the other hand, it has been unclear what material parameter is crucial for the superconducting nonlinear optical response. It is desirable to perform a comprehensive analysis of the superconducting nonlinear optical responses based on a canonical model.

To this end, we investigate the second-order nonlinear responses in superconductors with single-band model Hamiltonians [3]. Focusing on the role of antisymmetric spin-orbit coupling, we present a systematic study of the superconducting nonlinear optical responses. The superconductivity-induced nonlinear optical responses disappear under some conditions on pair potential, whereas the response arises with the coexistence of intraband and interband pairing. Our study identifies a basic ingredient in superconducting nonlinear optics and may cover a broad range of noncentrosymmetric superconductors such as heavy-fermion and two-dimensional superconductors [4].

[1] J. Orenstein *et al.*, *Annu. Rev. Condens. Matter Phys.* 12, 247 (2021).

[2] H. Watanabe *et al.*, *Phys. Rev. B* 105, 024308 (2022).

[3] H. Tanaka *et al.*, *arXiv* :2205.14445.

[4] *Non-Centrosymmetric Superconductors: Introduction and Overview*, edited by E. Bauer and M. Sigrest, *Lecture Notes in Physics* Vol. 847 (Springer, Berlin, 2012); Y. Saito *et al.*, *Nat. Phys.* 12, 144 (2016).

Keywords: nonlinear optical response, nonreciprocal response, noncentrosymmetric superconductors

Unusual Superconductivity in the Nodal-Line Semimetal NaAlSi

*Toshiya Ikenobe¹, Daigorou Hirai², Takahiro Yamada³, Hisanori Yamane³, Zenji Hiroi¹Institute for Solid State Physics, University of Tokyo (Japan)¹Department of Applied Physics, Nagoya University (Japan)²Institute of Multidisciplinary Research for Advanced Materials, Tohoku University (Japan)³

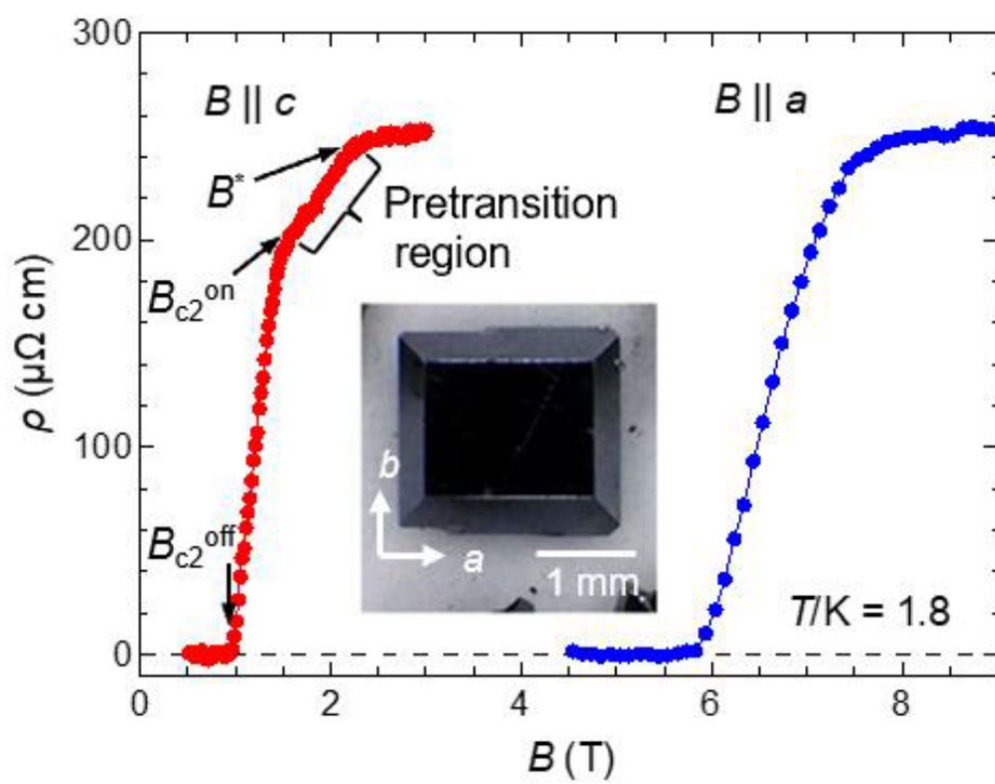
NaAlSi crystallizes in an anti-PbFCl-type layered structure [1] and exhibits superconductivity below $T_c = 6.8$ K [2,7]. The superconductivity seemed to be of the conventional *s*-wave type based on phonon-mediated Cooper pairing [3-6]. However, recent heat capacity measurements using single crystals of NaAlSi showed the possibility of a complex superconducting gap [7]. Interestingly, electronic state calculations showed that NaAlSi is a nodal-line semimetal [5,8,9], in which nontrivial topological surface states exist: a drumhead band at around the point in the (0 0 1) surface and a flat band along the line in the (1 0 0) surface [9].

We studied the resistive transitions under magnetic fields using plate-like single crystals of NaAlSi such as shown in Fig. 1. A significant reduction in resistivity was observed at a pre-transitional region ($B_{c2}^{on} - B^*$) above the bulk superconducting transition at $B_{c2}^{off} - B_{c2}^{on}$ only in the case that the magnetic field was perpendicular to the plane, not parallel to the plane (Fig. 1). No anomaly was observed at $T^*(B^*)$ in the heat capacity measurement, suggesting the existence of a fractional superconductivity different from the bulk superconductivity, although the details have not yet been clarified [10]. Meanwhile, the field dependence of the resistivity on the magnetic field parallel to the plate shows a sharp superconducting transition (Fig. 1), indicating that there is a field-angle dependence in resistive transition. In order to understand the origin of the fractional superconductivity, we measured the field dependence of the superconducting transition in electrical resistivity as a function of the magnetic field angle. We show the possibility that the fractional superconductivity has a two-dimensional character and suggest that it occurs at the crystal surface by measuring the current dependence of the transition.

Figure 1: Magnetic field dependence of the resistivity of a NaAlSi crystal at 1.8 K [7]. The red and blue curves are for $B \parallel c$ and a , respectively.

- [1] W. Westerhaus et al., Z. Naturforsch. B 34, 352 (1979).
- [2] S. Kuroiwa et al., Physica C 466, 11 (2007).
- [3] L. Schoop et al., Phys. Rev. B 86, 174522 (2012).
- [4] H. M. Tütüncü et al., Philos. Mag. 96, 1006 (2016).
- [5] L. Muechler et al., APL Materials 7, 121103 (2019).
- [6] H. Y. Wu et al., Phil. Mag. Lett. 99, 29 (2019).
- [7] T. Yamada et al., J. Phys. Soc. Jpn. 90, 034710 (2021).
- [8] L. Jin et al., J. Mater. Chem. C 7, 10694 (2019).
- [9] X. Yi et al., J. Mater. Chem. C 7, 15375 (2019).
- [10] D. Hirai et al., J. Phys. Soc. Jpn, 91, 024702 (2022).

Keywords: Superconductivity, Topological material, nodal-line semimetal



PC5-2

Superconducting properties and gap structure of the topological superconducting candidate Ti_3Sb

*Hendrik Hebbeker¹, Matt Smylie^{1,2}, Jared Dans¹, Ramakanta Chapai², Wai-Kwong Kwok², John Mitchell², Ulrich Welp²

Department of Physics and Astronomy, Hofstra University, USA¹
Materials Science Division, Argonne National Laboratory, USA²

We present a study of the superconducting properties of the candidate topological Ti_3Sb , an A15 material recently realized to have non-trivial band topology. We report magneto-transport and penetration depth measurements to ^3He temperatures and magnetization and calorimetry measurements to ^4He temperatures, finding all techniques agree on the superconducting phase boundary. The observed low-temperature upper critical field, ~ 5 T, is well short of estimated Ginzburg-Landau behavior. Penetration depth measurements reveal a full superconducting gap.

Work by MPS, JD, was in part supported by the U.S. Department of Energy, Office of Science, Office of Workforce Development for Teachers and Scientists (WDTS) under the Visiting Faculty Program (VFP). Work by RC, WKK, JFM, UW was supported by the US Department of Energy, Office of Science, Basic Energy Sciences, Materials Sciences and Engineering Division.

Keywords: Topological superconductor

Unusual transport properties with in-plane magnetic field in $\text{Sr}_x\text{Bi}_2\text{Se}_3$ single crystal*Yuhang Zu¹, Takumi Matsumae¹, Sunseng Pyon¹, Tsuyoshi Tamegai¹The University of Tokyo¹

Bi_2Se_3 is one of the representative topological insulators that show unique metallic surface state despite their insulating nature of the bulk. By doping Cu or Sr into Bi_2Se_3 , it becomes a topological superconductor, which shows novel properties such as nematicity [1]. In this study, we prepared high-quality single crystals of $\text{Sr}_x\text{Bi}_2\text{Se}_3$ and investigated its in-plane magnetic-field-angle dependence of resistivity. Resistivity (ρ) was measured with current along a -axis at 2 K by applying the in-plane magnetic field along the direction at an angle φ from a -axis. We have measured samples with nominal compositions $x = 0.04$ and 0.17 . Figures 1(a) and (c) show temperature dependences of magnetization in $\text{Sr}_{0.17}\text{Bi}_2\text{Se}_3$ and resistivity in $\text{Sr}_{0.04}\text{Bi}_2\text{Se}_3$, respectively, which show that sample with $x = 0.17$ is a superconductor with $T_c = 2.8$ K. Figures 1(b) and (d) show $\Delta\rho$ as a function of φ at 8.5 T, which is defined by $\Delta\rho \equiv \rho - \rho_0$. $\Delta\rho(\varphi)$ mainly shows two-fold symmetry, or in other words nematicity. In Fig. 1(c), we also plot a fitting curve of $\Delta\rho(\varphi)$ with $\Delta\rho(\varphi) = \rho_1\cos(\varphi + \alpha_1) + \rho_2\cos(2\varphi + \alpha_2)$, where the 2nd term originates from the nematicity, magnetoresistance, or misalignment of the field from the in-plane direction. The fact that the minimum value of the 2φ component is at $\varphi = 0^\circ$ strongly suggest that it is caused either by nematicity or by magnetoresistance. In the case of magnetoresistance, its magnitude should be proportional to the square of the transverse component of the field with respect to the current, $(B\sin(\varphi))^2$, which means that it is proportional to $\cos(2\varphi)$. One of the possible origins of the 1st term is the Hall effect for currents flowing along the c -axis as shown in Fig. 2. If this interpretation is correct, the Hall voltage should be zero at $\varphi = 0^\circ$ and π . However, the zero-value angle is offset by $\sim 35^\circ$ as shown in Fig. 1(b). Such a shift can be explained by the shift of effective locations of the two voltage terminals, V_+ and V_- . Namely, if locations of the effective voltage terminals are not parallel to a -axis, the zero-value position of the Hall effect should change. Fitting of $\Delta\rho(\varphi)$ of the sample with $x = 0.04$ with only $\cos(\varphi)$ and $\cos(2\varphi)$ terms was unsatisfactory. Instead, fitting with additional terms as $\Delta\rho(\varphi) = \rho_1\cos(\varphi + \alpha_1) + \rho_2\cos(2\varphi + \alpha_2) + \rho_3\cos(3\varphi + \alpha_3) + \rho_4\cos(4\varphi + \alpha_4)$ gave satisfactory result. However, physical origins of the 3rd and 4th terms are not clear at the present stage. The unusual Hall voltage due to current inhomogeneity may not have relationship with the superconductivity of $\text{Sr}_x\text{Bi}_2\text{Se}_3$, because even non-superconducting $\text{Sr}_x\text{Bi}_2\text{Se}_3$ with small x shows it. However, as x decreases, the amplitude of $\cos(\varphi)$ term decreases ($\text{Sr}_{0.17}\text{Bi}_2\text{Se}_3$: 8%, $\text{Sr}_{0.04}\text{Bi}_2\text{Se}_3$: 0.3%), which implies that there can be a critical value of x above which $\cos(\varphi)$ term appears. Samples with even smaller x will be measured to find the critical x value below which the $\cos(\varphi)$ term disappears and we will try to find out the possible physical origins of $\cos(3\varphi)$ and $\cos(4\varphi)$ terms by analyzing data on different samples at different temperatures and magnetic fields.

[1] Y. Pan *et al.*, *Sci. Rep.* 6, 28632 (2016).

Fig. 1. (a) Temperature dependence of magnetization and (b) in-plane magnetic-field-angle dependence of magnetoresistance $\Delta\rho = \rho - \rho_0$ at 2K and 8.5 T with $\rho_0 = 1.168$ m Ω cm in

$\text{Sr}_{0.17}\text{Bi}_2\text{Se}_3$. (c) Temperature dependence of resistivity and (d) in-plane magnetic-field-angle dependence of magnetoresistance $\Delta\rho = \rho - \rho_0$ at 2K and 8.5 T with $\rho_0=0.295 \text{ m}\Omega\text{cm}$ in $\text{Sr}_{0.04}\text{Bi}_2\text{Se}_3$.

Fig. 2 Possible current flow in the $\text{Sr}_x\text{Bi}_2\text{Se}_3$ single crystal. The current path along c -axis exists, which may be bent by obstacles.

Keywords: $\text{Sr}_x\text{Bi}_2\text{Se}_3$, topological superconductor, magneto-transport

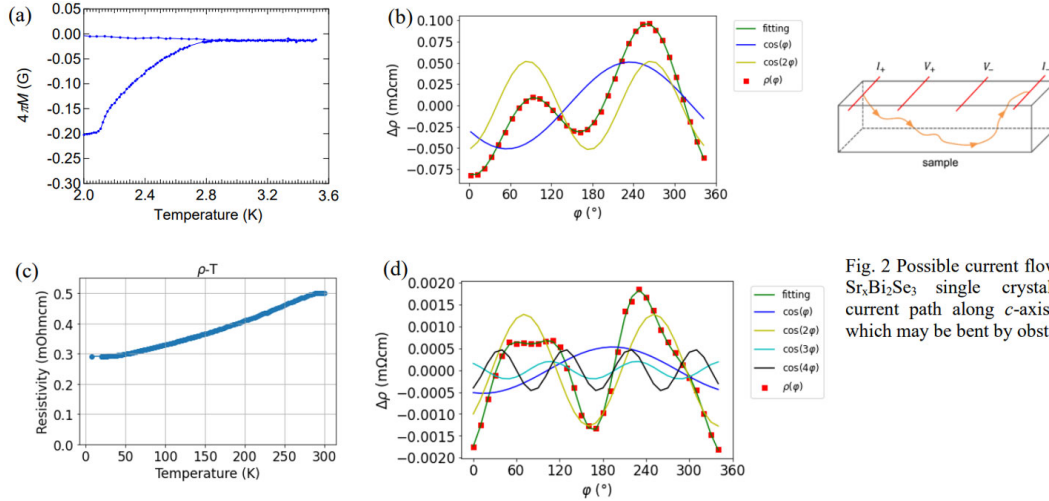


Fig. 1. (a) Temperature dependence of magnetization and (b) in-plane magnetic-field-angle dependence of magnetoresistance $\Delta\rho = \rho - \rho_0$ at 2K and 8.5 T with $\rho_0=1.168 \text{ m}\Omega\text{cm}$ in $\text{Sr}_{0.17}\text{Bi}_2\text{Se}_3$. (c) Temperature dependence of resistivity and (d) in-plane magnetic-field-angle dependence of magnetoresistance $\Delta\rho = \rho - \rho_0$ at 2K and 8.5 T with $\rho_0=0.295 \text{ m}\Omega\text{cm}$ in $\text{Sr}_{0.04}\text{Bi}_2\text{Se}_3$.

Fig. 2 Possible current flow in the $\text{Sr}_x\text{Bi}_2\text{Se}_3$ single crystal. The current path along c -axis exists, which may be bent by obstacles.

Effect of Bipartite Lattice on Topological Superconductivity in Two-Dimensional Quasicrystals

*Masahiro Hori^{1,2}, Ryo Okugawa², Takanori Sugimoto³, Takami Tohyama², K. Tanaka¹

University of Saskatchewan and quanTA, Canada¹

Tokyo University of Science, Japan²

Osaka University QIQB, Japan³

Symmetry-based analyses play an important role in the theory of topological superconductivity (TSC). In this regard, the effects of the symmetry of lattice structures on TSC provide our better understanding of TSC. Among various lattice structures, quasicrystals (QCs) have unique symmetry such as the five-fold rotational symmetry, which is forbidden in periodic lattices. TSC in two-dimensional quasicrystals has been investigated [1,2], where an s-wave TSC is realized in a Penrose tiling illustrated in Fig. 1. In the Penrose tiling, there are two sublattices that we denote A/B-sublattice. In the previous studies [1,2], it is assumed that the A- and B-sublattices have the same on-site potential. In real materials, however, such an assumption may not always be satisfied due to different local environments of sites in respective sublattices. Accordingly, we need to clarify the effect of bipartite lattice on TSC in quasicrystals.

In this study, we perform self-consistent calculation on the attractive Hubbard model with Zeeman field and Rashba spin-orbit coupling in a Penrose lattice. We introduce an on-site potential acting on A-sublattice sites, making A-sublattice and B-sublattice inequivalent. By changing the on-site potential, we calculate the topological invariant to classify the topology of the system. We find that topological phase transitions occur even in the presence of the on-site potential. We have thus confirmed that TSC can exist even when A-sublattice and B-sublattice are not equivalent in quasicrystals.

References:

- [1] R. Ghadimi, T. Sugimoto, K. Tanaka, T. Tohyama, Phys. Rev. B 104, 144511 (2021).
- [2] M. Hori et al., to be submitted.

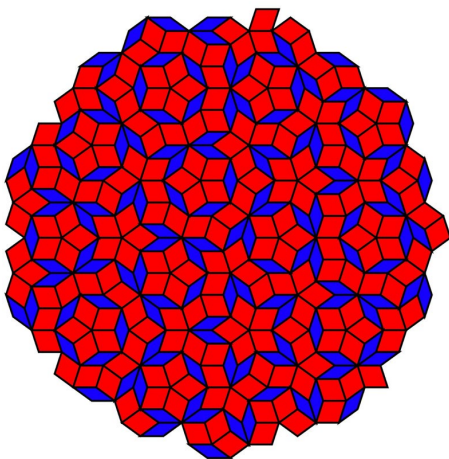


Figure Caption:
Fig. 1. Penrose QCs.

Keywords: Topological superconductivity,
Quasicrystals, Penrose tiling, Bipartite

PC6-1

Fast screening of REBa₂Cu₃O_{7-x} compositions (RE – Y, Yb) using combinatorial chemistry inkjet printing

*Cornelia Pop¹, Albert Queralto¹, Lasse Wichmann¹, Nerea Jimenez¹, Lavinia Saltarelli¹, Adria Pacheco¹, Susagna Ricart¹, Xavier Obradors¹, Teresa Puig¹

Materials Science Institute of Barcelona¹

Due to their interesting properties, high temperature superconductors, especially REBa₂Cu₃O_{7-x} (REBCO, RE=Y, Rare Earth) superconductors, are key materials for energy efficient technologies. One of the most studied REBCO material since its discovery, is YBCO, although other rare earths have risen interest, due to their potentially improved properties. Moreover, the Chemical Solution Deposition (CSD) methodology has been proven to be a promising low cost and scalable approach for coated conductor manufacturing process using reel-to-reel deposition techniques such as slot-die coating, dip coating and inkjet printing. Nevertheless, the slow growth rate of the standard CSD method for REBCO films growth (~1 nm/s) is a great limitation for the industrialization process. This limitation can be overcome by the recently developed CSD compatible method, the Transient Liquid Assisted growth – TLAG-CSD. In this method the epitaxial growth is controlled by the fast RE ions diffusion dissolved in a Ba-Cu-O transient liquid, leading to much faster growth rates (≈ 100-1000 nm/s) [1,2]. Being TLAG-CSD is a new methodology, many aspects need to be explored. One of these is the effect of different RE elements or RE mixers on the epitaxial growth kinetics, which implies a large time-consuming exploration of many process parameters. An appealing and practical approach are the new experimental techniques that are based on combinatorial chemistry and high-throughput experimentation (HTE). The objective of these techniques is to create large amounts of data by fabricating and characterizing material compositions and processing parameters in parallel, thus, increasing the speed and efficiency of the development process.

In this work we have used a drop-on-demand inkjet printing to prepare combinatorial samples [3] to achieve compositional gradients. In particular, we will here show results of Y_xYb_{1-x}BCO gradient samples obtained by printing selected patterns of two metalorganic inks (Y-Ba-Cu-O and Yb-Ba-Cu-O) by drop mixing, which afterwards are grown in particular conditions and characterized in parallel by means of XRD, SEM and EDX. We demonstrate that the versatility of drop-on-demand inkjet printing with independent multinozzle control is suitable for HTE of compositions and process conditions.

[1] Soler et al, *Nat Commun* 11, 344 (2020)

[2] S. Rasi et al, *Adv Sci* 2203834 (2022)

[3] A. Queralto, *ACS Appl. Mater. Interfaces*, 13, 9101 (2021)

Keywords: inkjet printing, superconductor inks, combinatorial chemistry, Transient Liquid Assisted growth – TLAG

Ozone Assisted Oxygenation of Transient Liquid Assisted Growth (TLAG) of $\text{YBa}_2\text{Cu}_3\text{O}_{7-\delta}$ films

*Aiswarya Kethamkuzhi¹, Lavinia Saltarelli¹, Kapil Gupta¹, Albert Queraltó¹, Diana García¹, Susagna Ricart¹, Joffre Gutierrez¹, Xavier Obradors¹, Teresa Puig¹

Instituto de Ciencia de Materiales de Barcelona (ICMAB-CSIC), Spain¹

High temperature superconductors (HTS) are one of the most ambitious achievements since the discovery of superconductivity and they have the potential to revolutionize large-scale applications in the form of coated conductors (CC). $\text{REBa}_2\text{Cu}_3\text{O}_{7-d}$ (REBCO, RE = Rare Earth) coated conductors which belong to the class of HTS called cuprates are one of the highly studied materials due to their exceptional superconducting properties. Although there are many material science and engineering challenges set forth in the fabrication of high performance CC. The novel growth method developed at ICMAB for the fabrication of REBCO films is an ultrafast (100-1000 nm/s) and cost effective technique which combines Chemical Solution Deposition (CSD) with a non-equilibrium Transient Liquid Assisted Growth (TLAG) method [1,2].

The superconducting properties of REBCO coated conductors are highly determined by its oxygen doping state. Therefore, oxygen incorporation into the REBCO lattice is an important step in the fabrication process. Optimally doped films have maximum T_c , but maximum critical current density, J_c can be achieved if one goes to the overdoped state where J_c increases as a consequence of an increase in condensation energy. This was demonstrated in TFA-CSD and PLD grown YBCO films oxygenated at lower temperatures [3]. It is expected that oxygenations at low temperatures will favour reaching the overdoped state, however then we need to cope with the low oxygen diffusion.

In this work, we want to overcome this challenge by using ozone assisted oxygenation in TLAG-YBCO films and study their superconducting properties and doping state. Optimization of ozone treatment based on the parameters ozone concentration, temperature, and dwell time will be presented. We demonstrate that the ozone assisted oxygenation has much faster kinetics compared to plane oxygen. The microstructural analysis from TEM measurements to understand the deleterious effect of high ozone concentrations is also included. Finally, we demonstrate the effect of ozone treatments in TLAG-YBCO nanocomposites.

[1] Soler, L., Jareño, J., Banchewski, J. et al. Ultrafast transient liquid assisted growth of high current density superconducting films. *Nat Commun* 11, 344 (2020)

[2] Rasi, Silvia, et al. "Kinetic Control of Ultrafast Transient Liquid Assisted Growth of Solution-Derived $\text{YBa}_2\text{Cu}_3\text{O}_{7-x}$ Superconducting Films." *Advanced Science*, 2022, p. 2203834.

[3] Stangl, A., Palau, A., Deutscher, G. et al. Ultra-high critical current densities of superconducting $\text{YBa}_2\text{Cu}_3\text{O}_{7-\delta}$ thin films in the overdoped state. *Sci Rep* 11, 8176 (2021).

PC6-3

In-situ X-ray synchrotron diffraction to understand the ultrafast growth mechanism of superconducting thin film

*Elzbieta Pach¹, Jordi Aguilar¹, Daniel Sanchez², Lavinia Saltarelli¹, Diana Garcia¹, Albert Queralto¹, Kapil Gupta¹, Eduardo Solano³, Marc Malfois³, Xavier Obrados¹, Teresa Puig¹

Institut de Ciència de Materials de Barcelona, ICMA-B-CESGA, Campus de la UAB, 08193 Bellaterra, Spain¹

GRMT, Department of Physics, University of Girona, E17071-Girona, Spain²

NCD-SWEET beamline, ALBA synchrotron, Carrer de la Llum 2-26, 08290 Cerdanyola del Vallès, Spain³

Solving the problem of scalable production methods for low-cost, efficient and flexible high temperature superconducting materials (HTS) compatible with Coated Conductors (CC) technology is one of the goals set for the Energy Transition. Nowadays, HTS based on REBa₂Cu₃O₇ (RE=Y or Rare Earth, REBCO) are manufactured as long, flexible conductors deposited on metallic substrates using thin film technologies, which are rather expensive. An alternative and highly innovative method, called Transient Liquid Assisted Growth (TLAG) [1] is used in our approach. It is a non-equilibrium process based on epitaxial crystallization from a transient melt at very high growth rates (100 nm/s, 100 times larger than conventional methods). This process is compatible with low cost, scalable chemical solution deposition methods and allows to grow high temperature epitaxial superconducting films. However, in order to better understand and control the process, determine the phases' evolution and the kinetic phase diagrams that would permit to better control the properties of as grown REBCO thin films, a new methodology had to be developed. This goal is being achieved through fast acquisition of in-situ X-Ray diffraction data during the TLAG process at the NCD-SWEET synchrotron beamline of ALBA synchrotron in Spain. For that purpose, a unique portable system was developed using a fast heating XRD furnace capable to rise the temperature up to 1000 °C at rates up to 300 °C/min and controlled atmosphere with total pressures from 10⁻⁵ bar to 1 bar while controlling the oxygen partial pressure and flow rate, all synchronized with simultaneous acquisition of 2D XRD images at 100 ms/image at 18 keV. Additionally, the system allows for simultaneous analysis of the volatiles with mass spectrometry and in-situ electrical conductivity that permits to follow the phase transformation from the insulating precursor phases to the metallic superconductor phase at the growth conditions. The ultrafast process of TLAG required very fast time responses of all the systems and accurate time synchronizations. Results on the epitaxial nucleation and growth mechanism of the REBCO phase on STO single crystals and metallic substrates, and TLAG phase evolutions process will be discussed.

[1] L. Soler et al, Nature Communications, 11, 344 (2020) * Research funded by ERC-2014-ADG-669504 and CSIC PTI-TRANSENER+

PC6-4-INV

Unusual Curie behavior and contributions from charge density waves in the in- and out-of-plane magnetization of underdoped $\text{YBa}_2\text{Cu}_3\text{O}_{6+x}$ crystals

*Ivan Kokanović¹

Department of Physics, Faculty of Science, University of Zagreb, Zagreb, Croatia.¹

In two recent papers [1, 2] we have shown how measurements of the static magnetic susceptibility of $\text{YBa}_2\text{Cu}_3\text{O}_{6+x}$ single crystals, $\chi_c(T)$ for magnetic fields applied along the c -axis and $\chi_{ab}(T)$ for fields in the ab -plane, can give useful information about their thermodynamic properties which are still being hotly debated. SQUID magnetometry above the superconducting (s/c) transition temperature T_c is used for larger crystals while piezolever torque magnetometry gives $\chi_c(T) - \chi_{ab}(T)$ for tiny crystals [2]. We briefly review the main results of this work - the T -dependent anisotropy well above T_c arises from the pseudogap and the g -factor anisotropy while at lower T there are Gaussian s/c fluctuations with a strong cut-off above $1.1 T_c$. Appropriate analysis allows the relatively small, but still important, Curie terms to be separated from other contributions to the susceptibility. Our data support a picture in which the Curie terms arise from oxygen disorder in the Cu-O chains. This agrees with published work on polycrystalline samples where the sample cooling rate was varied [3], but here we show that the Curie plots flatten out above 200 K. We identify small effects of charge density wave (CDW) instabilities in the temperature (T) derivative of the in-plane susceptibility $d\chi_{ab}(T)/dT$ and discuss their x dependence. We discuss some of these results in connection with a study [4] at higher magnetic fields up to 33 T. We then present some new data for heavily under-doped crystals with hole concentrations per CuO_2 plane, from $p = 0.058$ up to 0.073. This is the region where neutron scattering studies [5, 6] give evidence for competition between incommensurate magnetic short-range order and superconductivity. We have studied crystals with three values of x , measuring $\chi_c(T)$ and $\chi_{ab}(T)$ immediately after fixing x by quenching on to a copper block and again after allowing sufficient time at room temperature for the Cu-O chains to order. In this doping range, ordering the Cu-O chains increases T_c and substantially reduces the Curie term. The $\chi_D(T) = \chi_c(T) - \chi_{ab}(T)$ data show a weakly T -dependent linear region at higher T where $\chi_D(0)$ is $1-2 \times 10^{-4}$ emu/mol. We also discuss deviation from this linear behavior in terms of 2D or 3D Gaussian superconducting fluctuations at lower T .

References

- [1] I. Kokanović and J. R. Cooper, Phys. Rev. B 94, 075155 (2016).
- [2] I. Kokanović, et al., Phys. Rev. B 88, 060505(R) (2013).
- [3] J. Biscaras, et al., Phys. Rev. B 85, 134517 (2012).
- [4] Jing Fei Yu, et al., Phys. Rev. B 92, 180509(R) (2015).
- [5] D. Haug, et al., Phys. Rev. Lett. 103, 017001 (2009).
- [6] D. Haug, et al., New J. Phys. 12, 105006 (2010).

Keywords: Superconductivity, Magnetic properties, Strongly correlated systems

PC6-5-INV

Magnetotransport signatures of antiferromagnetism coexisting with charge order in the trilayer cuprate $\text{HgBa}_2\text{Ca}_2\text{Cu}_3\text{O}_{8+\delta}$

*Cyril Proust¹

LNCMI-Toulouse / CNRS¹

Multilayered cuprates possess not only the highest superconducting temperature transition but also offer a unique platform to study disorder-free CuO_2 planes and the interplay between competing orders with superconductivity. After a short introduction on multi-layered cuprate superconductors, I'll present a recent study of quantum oscillation and Hall effect in magnetic field up to 88 T in the underdoped trilayer cuprate $\text{HgBa}_2\text{Ca}_2\text{Cu}_3\text{O}_{8+\delta}$. A careful analysis of the complex spectra of quantum oscillations strongly supports the coexistence of multiple competing orders. In particular, our interpretation implies that a metallic antiferromagnetic state extends deep inside the superconducting phase, a key ingredient that supports magnetically mediated pairing interaction in cuprates.

Keywords: high T_c superconductor, electronic properties, high magnetic field

Charge density waves and Fermi surface reconstruction in the clean overdoped cuprate superconductor $\text{Ti}_2\text{Ba}_2\text{CuO}_{6+\delta}$

*Stephen Hayden¹, Charles Tam¹, Jake ≈ Ayres¹, Kurt Kummer², Flora Yakhou-Harris², John Cooper³, Anthony Carrington¹

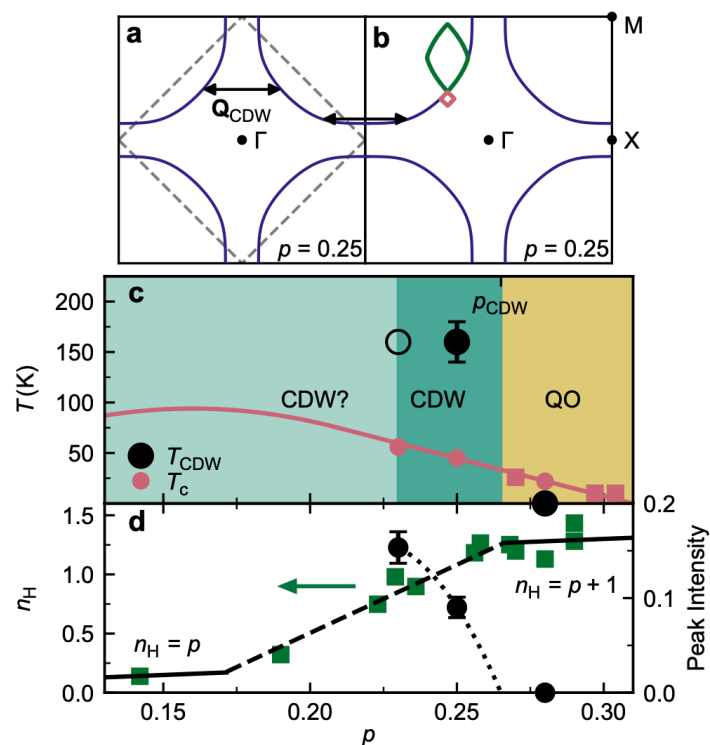
University of Bristol (United Kingdom)¹

ESRF, The European Synchrotron (France)²

University of Cambridge (United Kingdom)³

Hall effect and quantum oscillation measurements on high temperature cuprate superconductors show that underdoped compositions have small Fermi surface pockets whereas when heavily overdoped, a single much larger pocket is found. The origin of this change in electronic structure has been unclear, but may be related to the high temperature superconductivity. Here we show that the clean overdoped single-layer cuprate $\text{Ti}_2\text{Ba}_2\text{CuO}_{6+\delta}$ (TI2201) displays CDW order with a remarkably long correlation length $\xi \approx 200 \text{ \AA}$ which disappears above a hole doping of $p_{\text{CDW}} \approx 0.265$. We show that the evolution of the electronic properties of TI2201 as the doping is lowered may be explained by a Fermi surface reconstruction which accompanies the emergence of the CDW below p_{CDW} . Our results demonstrate importance of CDW correlations in understanding the electronic properties of overdoped cuprates. The figure shows (a) the Fermi surface of Th2201; (b) the phase diagram of overdoped TI2201 and (c) the doping dependence of the Hall number.

Keywords: superconductivity, charge density wave, Fermi surface reconstruction



PC7-1

Critical magnetic fields of superconductors with arbitrary potential and pair-breaking scattering

*Ruslan Prozorov¹, Vladimir G. Kogan¹

Ames National Laboratory¹

The upper critical magnetic field, H_{c2} , the nucleation field of surface superconductivity, H_{c3} , and the thermodynamic critical magnetic field, H_c , are evaluated within the weak-coupling theory for the isotropic s -wave pairing with arbitrary transport and pair-breaking scattering [1,2]. We find that the maximum ratio, $R=H_{c3}/H_{c2}$, reached for a magnetic field parallel to the surface, remains within $1.55 < R(T) < 2.34$, regardless of temperature or the scattering type. While the nonmagnetic impurities tend to flatten the $R(T)$ curve, magnetic scattering shifts the maximum of $R(T)$ to lower temperatures. Surprisingly, magnetic scattering has a milder impact on $R(T)$ than nonmagnetic scattering. The surface superconductivity is quite robust, the maximum ratio $R = 1.7$ is found even in the gapless state. Furthermore, we used Eilenberger's energy function to evaluate the condensation energy F_c and the thermodynamic critical magnetic field H_c for arbitrary temperature and scattering parameters. By comparing H_{c2} and H_c , we find that transport scattering promotes type-II behavior, but pair-breaking scattering pushes materials toward type-I superconductivity [3].

Finally, by conducting high precision and high-resolution calculations of F_c as a function of the pair-breaking scattering at very low temperatures we confirm the existence of a type-2.5 topological quantum phase transition from gapped to gapless state suggested recently from the discontinuity of the third derivative of F_c from the analytical Maki's solutions for F_c at $T=0$ [4]. Here we show the temperature dependence of the third derivative and the temperature broadening of this quantum critical point to a cone-like structure as observed for other quantum critical phase transitions.

References [1] V. G. Kogan and R. Prozorov, "Critical Fields of Superconductors with Magnetic Impurities", Phys. Rev. B 106, 054505 (2022).

[2] V. G. Kogan and R. Prozorov, "Changing the Type of Superconductivity by Magnetic and Potential Scattering", Phys. Rev. B 90, 180502 (2014).

[3] V. G. Kogan and R. Prozorov, "Anisotropic Criteria for the Type of Superconductivity", Phys. Rev. B 90, 54516 (2014).

[4] Y. Yerin, A. A. Varlamov, and C. Petrillo, "Topological Nature of the Transition between the Gap and the Gapless Superconducting States", EPL 138, (2022).

Keywords: upper critical field, third critical field, thermodynamic critical field, quantum topological phase transition

PC7-2-INV

Fermi surface transformation at the pseudogap critical point of a cuprate superconductor

*Yawen Fang¹, Gaël Grissonnanche^{1,2,3}, Anaëlle Legros^{3,4}, Simon Verret³, Francis Laliberté³, Clément Collignon³, Amirreza Ataei³, Maxime Dion³, Jianshi Zhou⁵, David Graf⁶, Michael J. Lawler^{1,7}, Paul A. Goddard⁸, Louis Taillefer^{3,9}, B. J. Ramshaw^{1,9}

Laboratory of Atomic and Solid State Physics, Cornell University, Ithaca, NY, USA¹

Kavli Institute at Cornell for Nanoscale Science, Ithaca, NY, USA²

Département de physique, Institut quantique, and RQMP, Université de Sherbrooke, Sherbrooke, Québec, Canada³

SPEC, CEA, CNRS-UMR 3680, Université Paris-Saclay, Gif-sur-Yvette, France⁴

Materials Science and Engineering Program, Department of Mechanical Engineering, University of Texas at Austin, Austin, TX, USA⁵

National High Magnetic Field Laboratory, Tallahassee, FL, USA⁶

Department of Physics, Applied Physics and Astronomy, Binghamton University, Binghamton, NY, USA⁷

Department of Physics, University of Warwick, Coventry, UK⁸

Canadian Institute for Advanced Research, Toronto, Ontario, Canada⁹

The nature of the pseudogap phase remains a major puzzle in our understanding of cuprate high-temperature superconductivity. Whether or not this metallic phase is defined by any of the reported broken symmetries, the topology of its Fermi surface remains a fundamental open question. Here we use angle-dependent magnetoresistance (ADMR) to measure the Fermi surface of the $\text{La}_{1.6-x}\text{Nd}_{0.4}\text{Sr}_x\text{CuO}_4$ cuprate. Outside the pseudogap phase, we fit the ADMR data and extract a Fermi surface geometry that is in excellent agreement with angle-resolved photoemission data. Within the pseudogap phase, the ADMR is qualitatively different, revealing a transformation of the Fermi surface. We can rule out changes in the quasiparticle lifetime as the sole cause of this transformation. We find that our data are most consistent with a pseudogap Fermi surface that consists of small, nodal hole pockets, thereby accounting for the drop in carrier density across the pseudogap transition found in several cuprates.

Keywords: Fermi surface, pseudogap, cuprate superconductor

PC7-3-INV

Unconventional spectral signature of T_c in a pure d -wave superconductor

*Makoto Hashimoto¹

SLAC National Accelerator Laboratory¹

Angle-resolved photoemission spectroscopy (ARPES) has been an important tool to study the electronic phase diagram of high- T_c cuprate superconductors [1]. With the recent instrumentation improvements, ARPES measurements in the normal state with unprecedented precision became possible, revealing that the incoherent strange metal abruptly reconstructs into a more conventional metal with quasiparticles across the putative critical doping around 19%, concomitant with the collapse of the pseudogap, defining a temperature-independent vertical phase boundary [2]. In this talk, we focus on the overdoped regime above such critical doping to study the spectroscopic signature of superconducting fluctuations above T_c . Combined with theoretical calculations, the result suggests that the antinodal shallow band bottom is playing an important role for the fluctuating superconductivity [3]. Furthermore, we demonstrate that ARPES-derived electronic specific heat reproduces the specific heat peak at T_c , making direct connection between ARPES spectra and thermodynamic property [4]. We show that this thermodynamic anomaly arises from the singular growth of in-gap spectral intensity across T_c with strong superconducting phase fluctuation.

[1] M. Hashimoto, I. M. Vishik, R.-H. He, T. P. Devereaux, Z.-X. Shen, *Nat Phys* 10, 483 (2014)

[2] S.-D. Chen*, M. Hashimoto* *et al.*, *Science* 366, 1099 (2019)

[3] Y. He *et al.*, *Phys Rev X* 11, 031068 (2021)

[4] S.-D. Chen*, M. Hashimoto* *et al.*, *Nature* 601, 562 (2022)

Keywords: High- T_c cuprates, ARPES

Muon Spin Relaxation Study of the Fe-substitution Effects
on Ferromagnetic Fluctuations in the Heavily Overdoped Bi-2201 Cuprates

*Yota Komiyama¹, Shusei Onishi¹, Hideki Kuwahara¹, Haruhiko Kuroe¹, Koshi Kurashima², Takayuki Kawamata³, Yoji Koike², Dita Puspita Sari^{4,5}, Isao Watanabe⁵, Tadashi Adachi¹

Department of Engineering and Applied Sciences, Sophia University, Japan¹

Department of Applied Physics, Tohoku University, Japan²

Department of Natural Sciences, Tokyo Denki University, Japan³

College of Engineering, Shibaura Institute of Technology, Japan⁴

Meson Science Laboratory, RIKEN Nishina Center, Japan⁵

In the high- T_c cuprate superconductivity, the relationship between antiferromagnetic (AF) spin fluctuations and superconductivity has been extensively studied. It has been suggested that low-energy AF fluctuations disappear concomitant with the suppression of superconductivity in the overdoped regime.¹⁾ On the other hand, resonant inelastic X-ray scattering has revealed robust AF fluctuations in the non-superconducting heavily overdoped (HOD) regime.²⁾

It has been proposed that ferromagnetic (FM) fluctuations exist and are related to the suppression of superconductivity in the HOD regime of high- T_c cuprates.^{3,4)} There are two candidates for the origin of FM fluctuations. One is itinerant electron ferromagnetism due to enhanced spin susceptibility at $q \sim (0, 0)$ and large density of states at the Fermi level.^{5,6)} The other is the double exchange interaction due to the multiband nature of the $\text{Cu}3d_{x2-y2}$ and $\text{Cu}3d_{3z2-r2}$ orbitals suggested by the Compton scattering.⁷⁾

Our former studies of the overdoped and HOD Bi-2201 cuprates revealed that FM fluctuations exist and were enhanced by the Fe-substitution.^{8,9)} To further understand the details of FM fluctuations, we performed muon-spin-relaxation (μSR) measurements of Fe-substituted Bi-2201.

Figure (a) shows zero-field μSR time spectra of 9.6% Fe-substituted $\text{Bi}_{1.74}\text{Pb}_{0.38}\text{Sr}_{1.88}\text{Cu}_{1-y}\text{Fe}_y\text{O}_{6+\delta}$ with $y = 0.096$ in the HOD regime. It is found that fast relaxation and muon-spin precession are observed at 4.1 K, suggesting the formation of a long-range magnetic order. Figure (b) shows the temperatures dependence of the relaxation rate of muon spins λ in HOD $\text{Bi}_{1.74}\text{Pb}_{0.38}\text{Sr}_{1.88}\text{Cu}_{1-y}\text{Fe}_y\text{O}_{6+\delta}$ with $y = 0, 0.05, 0.096$. It is found that λ is enhanced and exhibits a peak at low temperatures for the Fe-substituted samples. The peak temperature below which the spin-glass state is formed increases with Fe substitution.

For $y = 0.096$, the internal magnetic field at the muon site is comparable to that reported in the overdoped regime of Bi-2201 in which the AF order is formed around Fe.¹⁰⁾ We propose the formation of a cluster spin-glass at low temperatures, in which a short-range magnetic order is formed in a cluster around each Fe and a spin-glass state is formed between clusters in the CuO_2 plane. In the clusters, an AF order might be formed according to the overdoped regime.¹⁰⁾ On the other hand, based on our results, a FM order might be formed in the cluster.

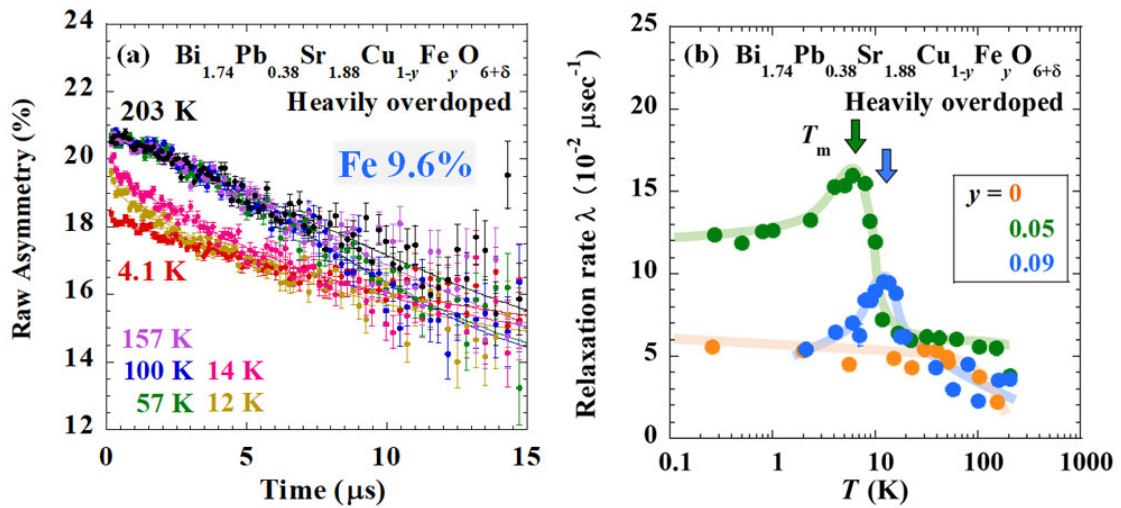
[1] S. Wakimoto *et al.*, Phys. Rev. Lett. 92, 217004 (2004).

[2] M. P. M. Dean *et al.*, Nat. Mater. 12, 1019 (2013).

- [3] A. Kopp *et al.*, Proc. Natl. Acad. Sci. U.S.A. 104, 6123 (2007).
- [4] J. E. Sonier *et al.*, Proc. Natl. Acad. Sci. U.S.A. 107, 17131 (2010).
- [5] Y. Y. Peng *et al.*, Phys. Rev. B, 98, 144507 (2018).
- [6] T. A. Maier and D. J. Scalapino, J. Supercond. Nov. Magn. 33, 15 (2020).
- [7] Y. Sakurai *et al.*, Science 332, 698 (2011).
- [8] K. Kurashima *et al.*, Phys. Rev. Lett. 121, 057002 (2018).
- [9] Y. Komiyama *et al.*, J. Phys. Soc. Jpn. 90, 084701 (2021).
- [10] H. Hiraka *et al.*, Phys. Rev. B 81, 144501 (2010).

Figure: (a) Zero-field μ SR time spectrum of HOD $\text{Bi}_{1.74}\text{Pb}_{0.38}\text{Sr}_{1.88}\text{Cu}_{1-y}\text{Fe}_y\text{O}_{6+\delta}$ with $y = 0.096$.
 (b) Temperature dependence of the relaxation rate of muon spins λ in HOD $\text{Bi}_{1.74}\text{Pb}_{0.38}\text{Sr}_{1.88}\text{Cu}_{1-y}\text{Fe}_y\text{O}_{6+\delta}$ with $y = 0, 0.05, 0.096$.

Keywords: Ferromagnetic fluctuations, Bi-2201, Heavily overdoped regime, Muon spin relaxation



PC7-5

Overdoped cuprates: conventional or exotic?

*Jeffery L Tallon¹

Victoria University of Wellington¹

Underdoped cuprates are without doubt complex and exotic. Several correlated states compete near the Fermi surface including superconductivity, charge ordering and the pseudogap 'state'. But for a long time it was thought that overdoped cuprates represented progressively more conventional behaviour - despite the fact that it has been known since quite early that there is a strong suppression of superfluid density as one progresses deeper into the overdoped state. We know that underdoped cuprates also display a suppression of superfluid density due to the pseudogap so this overdoped behaviour came to be known as the 'boomerang effect'. We have found this deeply puzzling because many other overdoped superconducting properties display conventional behaviour. Amongst these are the scaled BCS ratios for the condensation energy, the specific heat jump and the superconducting energy gap. So why should the superfluid density be increasingly suppressed with overdoping when e.g. the condensation energy is not? Techniques for measurement of superfluid density include muon spin relaxation, optics, susceptibility, mutual inductance and the tunnel diode resonator. We have been involved in a number of these earlier reports. But here we measure the superfluid density using field-dependent specific heat measurements on bulk samples of Ca-doped $\text{YBa}_2\text{Cu}_3\text{O}_x$ and $\text{Bi}_2\text{Sr}_2\text{CaCu}_2\text{O}_{8+x}$ and find no suppression of the superfluid density across the overdoped region, consistent with our earlier thermodynamic results mentioned above. Are the overdoped cuprates in this sense conventional after all? And what is the reason for these divergent results amongst so many different techniques? The cuprates continue to fascinate in their rich behaviour.

Keywords: Overdoped cuprates, superfluid density, field-dependent specific heat, condensation energy

PC7-6

Reduction Effects in the Electron-Doped High- T_c Cuprates Pr_2CuO_4 Single Crystal Studied by X-ray Absorption Fine Structure and Transport Property

*Riku Okada¹, Yusuke Nagakubo¹, Takashi Udagawa¹, Eri Takagaki¹, Koki Kawabata¹, Hideki Kuwahara¹, Motofumi Takahama², Takanori Taniguchi², Shun Asano², Kenji Ishii³, Daiju Matsumura⁴, Takuya Tsuji⁴, Masaki Fujita², Tadashi Adachi¹

Department of Engineering and Applied Sciences, Sophia University, Kioi-cho, Tokyo 102-8554, Japan¹

Institute for Materials Research, Tohoku University, Katahira, Sendai 980-8577, Japan²

Synchrotron Radiation Research Center, National Institutes for Quantum Science and Technology, Sayo, Hyogo 679-5148, Japan³

Materials Sciences Research Center, Japan Atomic Energy Agency, Sayo, Hyogo 679-5148, Japan⁴

In high temperature cuprate superconductors, doping carriers into parent antiferromagnetic (AF) Mott insulators destroys the AF order and brings about the superconductivity. In 2009, it has been reported that the superconductivity appears in a parent compound and in a wide range of electron concentration through the appropriate reduction of excess oxygen in the so-called T' -type thin films [1] and polycrystals [2], resulting in a phase diagram different from the well-known one. To investigate the superconductivity in the parent T' -cuprates, we performed measurements of the ab-plane electrical resistivity ρ_{ab} , Hall resistivity and Cu K-edge X-ray absorption fine structure (XAFS) using parent T' - Pr_2CuO_4 single crystals. Pr_2CuO_4 single crystals were reduced by the protect annealing [3], followed by the low-temperature [4] and dynamic annealing [5]. XAFS measurements were conducted at BL14B1 in SPring-8, Japan.

Figure shows the difference XAFS spectra of Pr_2CuO_4 reduced in vacuum at 10^{-5} Pa. For the protect annealed sample, the absorption intensity around 8981 eV, corresponding to the formation of Cu^+ [6], is large, and the additional low-temperature and dynamic annealing brings about further increase of the absorption intensity. These suggest that electrons are doped by the reduction annealing due to the removal of excess oxygen. Comparing the protect annealing at 10^{-5} Pa and 10^{-4} Pa, the amount of oxygen deficiency and electron doping were larger at 10^{-4} Pa. ρ_{ab} and Hall resistivity revealed that the sample annealed at 10^{-4} Pa is more conductive than 10^{-5} Pa. These suggest that Pr_2CuO_4 becomes conductive by the oxygen deficiency and electron doping.

[1] O. Matsumoto *et al.*, *Physica C* 469, 924 (2009).

[2] T. Takamatsu *et al.*, *Appl. Phys. Express* 5, 073101 (2012).

[3] T. Adachi *et al.*, *J. Phys. Soc. Jpn.* 82, 063713 (2013).

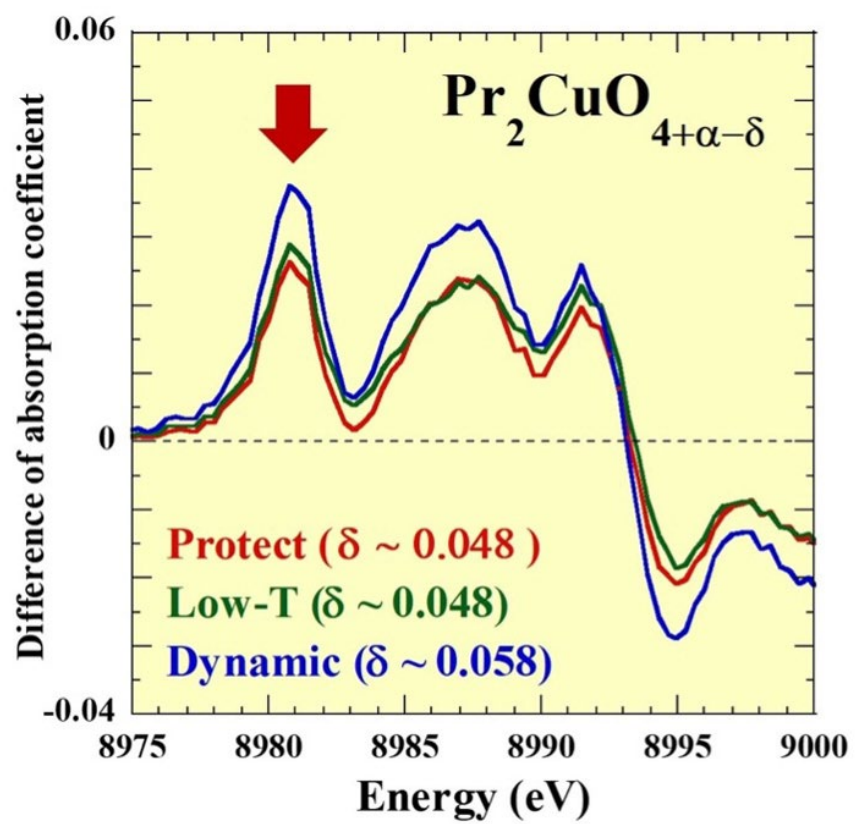
[4] Y. Krockenberger *et al.*, *Sci. Rep.* 3, 2235 (2013).

[5] Y. L. Wang *et al.*, *Phys. Rev. B* 80, 094513 (2009).

[6] S. Asano *et al.*, *J. Phys. Soc. Jpn.* 87, 094710 (2018).

Keywords: T' -type Cuprate Superconductor, X-ray absorption fine structure, Electrical

Resistivity, Hall Resistivity



PC7-7

Magnetic alignment behavior of DyBa₂Cu₃O_y grains controlled by annealing

*Shintaro Adachi¹, Ataru Ichinose², Walid Bin Ali¹, Fumiko Kimura¹, Jun-ichi Shimoyama³, Shigeru Horii¹

Kyoto University of Advanced Science¹

Central Research Institute of Electric Power Industry²

Aoyama Gakuin University³

To achieve high self-field and in-field critical current densities in the high critical temperature (high- T_c) cuprate superconductors, densification of the crystal texture and bi- or tri-axial crystal orientation are necessary. Here we are focusing on magnetic alignment as a method for triaxial orientation of REBa₂Cu₃O_y (RE123) grains. By using a magnetic field, we can orient crystal grains without touching the sample. The typical advantages of magnetic alignment are the needless highly oriented templates, and it is also the room temperature process.

At the structural phase transition from tetragonal to orthorhombic, RE123 forms twin microstructures in the grain level [1]. In the RE123 grain level, the $a(b)$ and $b(a)$ axes are orthogonal between the two adjacent domains. Such domains are separated by the (110) plane, as shown schematically in Figure 1. Therefore, the abundance ratio of domains may determine the in-plane magnetic anisotropy in the grain level. Magnetic anisotropy in the grain level is one of the important parameters that determine the energy of magnetic alignment. Recently, we fabricated biaxially aligned samples of DyBa₂Cu₃O_y (Dy123) powders by magnetic alignment. The Dy123 shows a relatively large magnetic anisotropy among RE123 cuprates. Furthermore, by observing transmission electron microscopy (TEM) images of a biaxially aligned Dy123 grain, we discovered the inhomogeneous domain ratio with twin microstructures contributing to in-plane magnetic anisotropy in the grain level [2]. As a next step, we are now investigating the possibility of controlling the in-plane magnetic anisotropy in the grain level of Dy123 by applying several annealing conditions. The enhancement of the in-plane domain ratio, including the twin microstructures by the annealing, leads to the enhancement of the in-plane magnetic anisotropy in the grain level. Thus, the annealing of Dy123 may reduce the magnitude of the magnetic field for magnetic alignment.

If the magnetic alignment of RE123 can be achieved by the magnetic field due to only the permanent magnets, it will be possible to support continuous fabrication processes by using the recently developed linear drive type of modulated rotating magnetic field system [5]. The purpose of this study is to improve the in-plane magnetic anisotropy of Dy123 in the grain level by annealing. Based on the above background, we investigated the annealing conditions for Dy123.

First, we obtained Dy123 polycrystals by sintering Dy123 pellets in air at 950°C with furnace cooling. And then, we also prepared Dy123 by controlling the oxygen content y by various annealings. Figure 2 shows the oxygen content y dependence of T_c for Dy123. For comparison, the oxygen content y dependence of T_c for Y123 [4] was also plotted. Due to the difference in RE ion species, the difference was observed in y - T_c plots. Dy123 has a narrower range of y in the $T_c = 90\text{K}$ phase than Y123. It was also suggested that Dy123 has a narrower range of y in the Ortho-2 phase than Y123. Dy123 will be in the Ortho-1 phase

when the oxygen content is $6.35 < y < 6.90$. A boundary between the Tetra- and Ortho-1 phases of Dy123 was also shown by the recent in-situ XRD experiment [5] to exist at y around 6.35. Based on these experimental results, we obtained Ortho-Dy123 samples from high-temperature phase Tetra-Dy123 by various annealing conditions. Ortho-Dy123 powder samples for magnetic alignment were biaxially aligned in epoxy resin under various modulated rotating magnetic fields. By solidifying the epoxy resin, the biaxially aligned Dy123 grains were fixed. Powder XRD and pole figure measurement were used to evaluate the degree of orientation of the sample.

In this presentation, we will report the details of our experimental results and discuss the relationship between the annealing conditions and the magnetic alignment behaviors of Dy123 grains.

[Acknowledgement] This work was partly supported by JSPS KAKENHI Grant Number JP17H03235

- [1] R. H. Hammond and R. Bormann, *Physica C* 162-164, 703 (1989).
- [2] S. Adachi et al., *IEEE-TAS* 32, 7200105 (2022).
- [3] S. Horii et al., *J. Cer. Soc. Jpn.* 126, 885 (2018).
- [4] R. J. Cava et al., *Physica C* 165, 419 (1990).
- [5] F. Kimura et al., *CrystEngComm* 24, 3807 (2022).

Keywords: cuprate superconductor, magnetic alignment, modulated rotating magnetic field, twin microstructures

Fig. 1

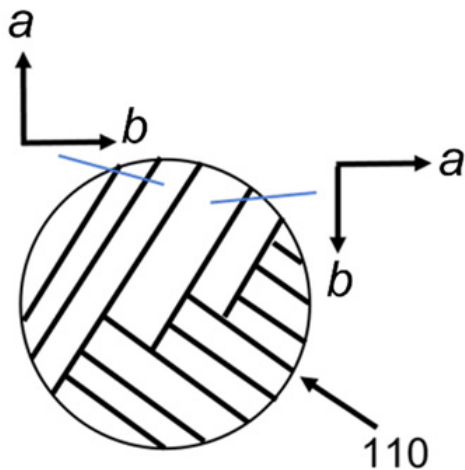
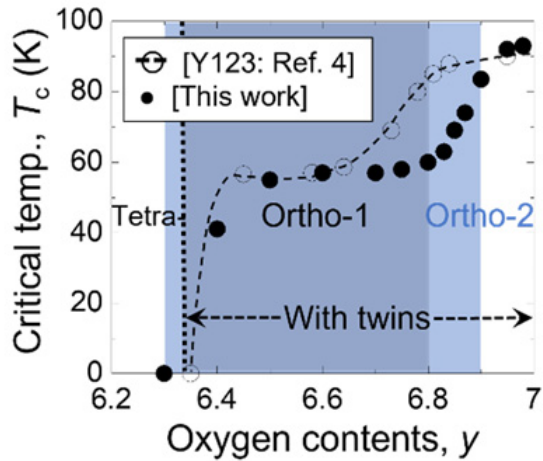


Fig. 2



PC8-1-INV

Interplay between superconductivity and magnetic fluctuations in iron pnictide $\text{RbEuFe}_4\text{As}_4$

*Alexei E Koshelev¹, David Collomb², Simon J Bending², Matthew P Smylie^{1,3}, Liam Farrar², Jin-Ke Bao^{1,4}, Duck Y Chung¹, Mercouri G Kanatzidis^{1,5}, Wai-K. Kwok¹, Ulrich Welp¹

Materials Science Division, Argonne National Laboratory, 9700 South Cass Avenue, Lemont, Illinois 60439, USA¹

University of Bath, Claverton Down, Bath BA2 7AY, United Kingdom²

Department of Physics and Astronomy, Hofstra University, Hempstead, New York 11549, USA³

Shanghai University, 99 Shangda Road, BaoShan District, Shanghai 200444 China⁴

Department of Chemistry, Northwestern University, Evanston, Illinois 60208, USA⁵

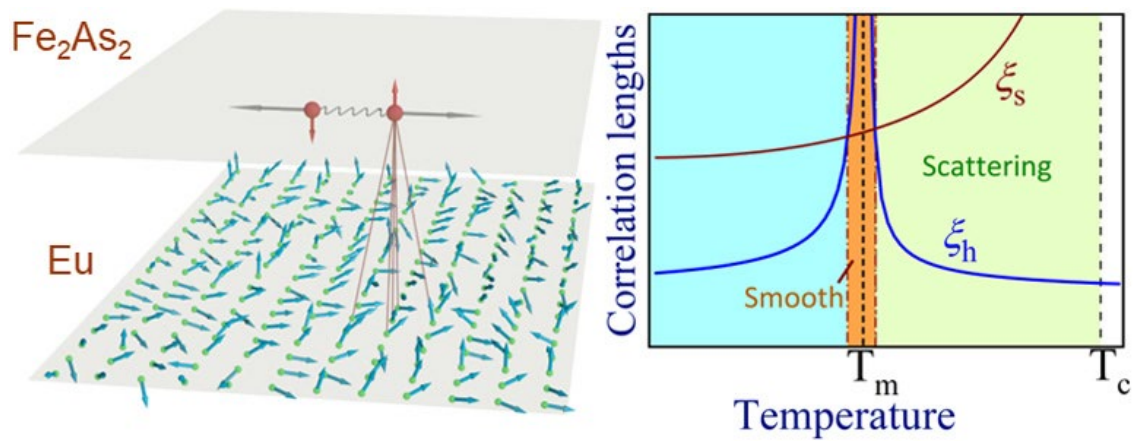
In spite of antagonism between magnetism and superconductivity, several known superconducting compounds host sublattices of rare-earth local magnetic moments which order inside superconducting state and weakly interact with Cooper pairs. In this situation, the local moments most strongly suppress superconductivity near the magnetic transition, in the regime of strong magnetic fluctuations. A notable example of such a material is iron pnictide $\text{RbEuFe}_4\text{As}_4$ with the superconducting transition at 36.7 K and the magnetic transition at 15 K. As a model for this material, we consider a clean layered superconductor containing magnetic-moments layers in which a magnetic order establishes inside a superconducting state without destruction of superconductivity. We investigate the corrections to the superconducting gap and London penetration depth caused by weak exchange interactions between magnetic and superconducting layers in the regime of correlated magnetic fluctuations [1], as illustrated in the Figure. The influence of nonuniform exchange field on superconducting parameters is very sensitive to the relation between the magnetic correlation length, ξ_h , and superconducting coherence length ξ_s defining the 'scattering' ($\xi_h < \xi_s$) and 'smooth' ($\xi_h > \xi_s$) regimes, see Figure. We quantified this 'scattering-to-smooth' crossover for the case of quasi-two-dimensional magnetic fluctuations realized in $\text{RbEuFe}_4\text{As}_4$. In the 'scattering' regime, the suppression of superconductivity is similar to the case of magnetic impurities [2] and the exchange corrections are proportional to the magnetic scattering rate, which grows linearly with ξ_h until it remains smaller than ξ_s . In the opposite limit, when ξ_h exceeds ξ_s , smoothing of spatial variations of the exchange field strongly diminishes its effect on superconducting parameters. The crossover between the regimes occurs to be unexpectedly broad: the scattering approximation becomes inaccurate already when ξ_h is substantially larger than ξ_s . We applied the developed theoretical framework to modelling the observed behavior of the London penetration depth extracted from the vortex imaging in $\text{RbEuFe}_4\text{As}_4$ [3]. Unexpectedly, we found that the exchange interaction between the magnetic and superconducting subsystems is quite noticeable and leads to strong suppression of the superfluid density near the magnetic transition.

Acknowledgements: This work was supported by the US Department of Energy, Office of Science, Basic Energy Sciences, Materials Sciences and Engineering Division.

References:

- [1] A. E. Koshelev, "Suppression of superconducting parameters by correlated quasi-two-dimensional magnetic fluctuations", Phys. Rev. B 100, 014518 (2019).
- [2] A. A. Abrikosov and L. P. Gor'kov, "Contribution to the theory of superconducting alloys with paramagnetic impurities", Sov. Phys. JETP 12, 1243 (1961); S. Skalski, O. Betbeder-Matibet, and P. R. Weiss, "Properties of superconducting alloys containing paramagnetic impurities", Phys. Rev. 136, A1500 (1964); V. G. Kogan, R. Prozorov, and V. Mishra, "London penetration depth and pair breaking", Phys. Rev. B 88, 224508 (2013).
- [3] D. Collomb et al., "Observing the suppression of superconductivity in RbEuFe₄As₄ by correlated magnetic fluctuations", Phys. Rev. Lett. 126, 157001 (2021).

Keywords: Magnetic superconductors, Iron pnictides



PC8-2

The effects of suppressing Eu magnetic order via 20% Ca doping in single crystals of the magnetically ordered superconductor $\text{RbEu}_{1-x}\text{Ca}_x\text{Fe}_4\text{As}_4$

*Matt Smylie^{1,2}, Ramakanta Chapai², Hendrik Hebbeker¹, Jared Dans¹, Angelo Patrizi¹, Jinke Bao², Duck Young Chung², Mercouri Kanatzidis^{2,3}, John Singleton⁴, Fedor Balakirev⁴, Wai-Kwong Kwok², Ulrich Welp²

Department of Physics and Astronomy, Hofstra University, USA¹

Materials Science Division, Argonne National Laboratory, USA²

Department of Chemistry, Northwestern University, USA³

National High Magnetic Field Laboratory, Los Alamos National Laboratory, USA⁴

We investigate the effect of Ca-for-Eu doping in single crystals of the magnetic superconductor $\text{RbEuFe}_4\text{As}_4$ at 20% doping, observing a ~ 1.5 K suppression of the magnetic ordering temperature with no effect on T_c . Upper critical fields measured conventionally and via pulsed-field techniques are similar to the undoped compound. At low temperature below the ferromagnetic saturation field, we find evidence of a field-induced transition to a new magnetic state not seen in the $x = 0$ compound. Additionally, there is a pronounced effect on the superconducting critical current measured via magnetic hysteresis loops not previously observed.

Work by MPS, JD, was in part supported by the U.S. Department of Energy, Office of Science, Office of Workforce Development for Teachers and Scientists (WDTS) under the Visiting Faculty Program (VFP). Work by RC, JKB, DYC, MGK, WKK, UW was supported by the US Department of Energy, Office of Science, Basic Energy Sciences, Materials Sciences and Engineering Division. A portion of this work was performed at the National High Magnetic Field Laboratory, which is supported by National Science Foundation Cooperative Agreements No. DMR-1157490 and No. DMR-1644779, and the State of Florida, as well as the Strongly Correlated Magnets thrust of the DoE BES "Science of 100 T" program.

Keywords: Magnetic superconductor, Ferromagnetic superconductor

Microstrips fabrication of iron-based superconductor NdFeAs(O,H) and their transport properties

*Atsuro Yoshikawa¹, Hiroya Imanaka¹, Hiroto Hibino¹, Takafumi Hatano¹, Hiroshi Ikuta¹

Department of Materials Physics, Nagoya University, Japan¹

Single photon detectors (SPDs) are key components in various applications such as quantum key distribution, satellite laser ranging, and fluorescence lifetime measurement. Recently, SPDs based on superconducting nanowires (SSPDs) are gathering extensive research interests, since SSPDs show excellent performances, in terms of detection efficiency, detection speed, and time resolution [1]. To achieve high performances, fabrication of superconducting strips with line widths down to about 100 nm is required. However, such nanofabrication tends to result in serious degradation of the superconducting properties. Indeed, the operating temperature of SSPDs based on NbN, which is one of the most studied materials for SSPDs, is generally restricted to 2~3 K, much lower than the critical temperature (T_c) of bulk NbN ($T_c = 16$ K).

Using a high- T_c superconductor could increase the operating temperature of SSPDs. We have investigated the microfabrication of NdFeAs(O,F), which shows the highest T_c among the iron-based superconductors. We have fabricated NdFeAs(O,F) thin films into micro-bridges with line widths down to 0.84 μm [2], and found that T_c was not much affected. This suggests that NdFeAs(O,F) has a great potential for SSPD applications. However, to fabricate a NdFeAs(O,F) thin film, it is necessary to deposit a NdOF layer on the top, which serves as the source of F [3]. This NdOF layer would become an obstacle for photon detection. Recently, it has become possible to grow NdFeAs(O,H) thin films, which have T_c 's as high as NdFeAs(O,F). Furthermore, it is not necessary to deposit another layer on the film to obtain a superconducting film, which is more suitable for SSPD applications. In this work, therefore, we fabricated NdFeAs(O,H) microstrips with line widths down to about 1 μm and evaluated their transport properties.

The parent NdFeAsO thin film was grown on a MgO (001) substrate by molecular beam epitaxy [3]. After the growth, the film was sealed in an evacuated quartz tube filled with CaH₂ powder (~0.8 g) and heated at 510 °C for 36 h to substitute H for O by a topotactic reaction $\text{NdFeAsO} + (x/2)\text{CaH}_2 \rightarrow \text{NdFeAsO}_{1-x}\text{H}_x + (x/2)\text{CaO}$ [4]. The obtained NdFeAs(O,H) thin film was patterned by conventional photolithography and Ar-ion dry etching using a reactive ion etcher (Ar-RIE). During the Ar-RIE process, the sample is exposed to Ar plasma, which may cause damages to the strip lines. Hence, we carefully optimized the etching conditions to minimize the decrease in T_c .

Figure (a) shows the line width dependence of T_c of NdFeAs(O,H) microstrips (red squares). T_c of the strip lines (T_c^{line}) were normalized by that of the film measured before etching (T_c^{film}). For comparison, the data of NdFeAs(O,F) microstrips [2] are plotted by black circles. T_c^{line} of NdFeAs(O,H) was generally higher than 85% of T_c^{film} down to line width of 1 μm , similarly to NdFeAs(O,F). Figure (b) shows the line width dependence of J_c of NdFeAs(O,H) (red squares) and NdFeAs(O,F) (black circles). It can be seen that there is a decrease in J_c when the line width was 2 μm or less, which was also observed for NdFeAs(O,F). This indicates that the damages caused by the Ar-RIE process was not completely suppressed. Nevertheless, J_c

remained high and was more than 1 MA/cm² down to about 1 μm.

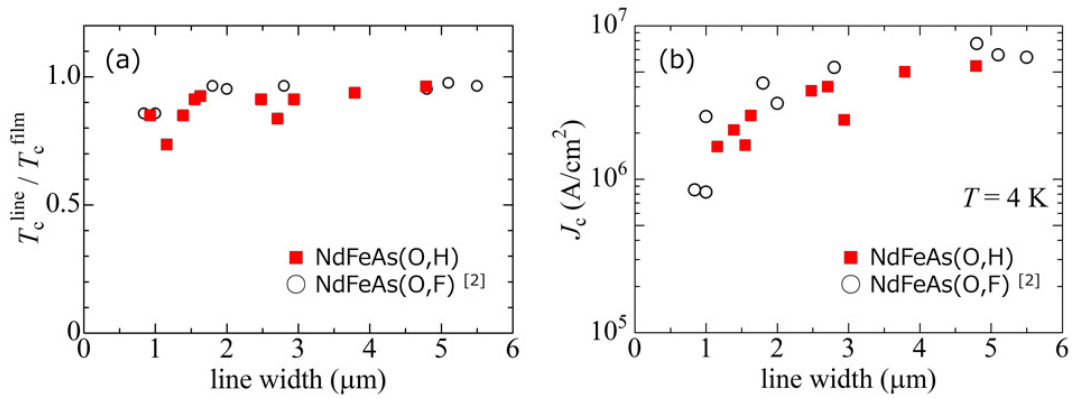
References

- [1] C. M. Natarajan *et al.*, Supercond. Sci. Technol. 25, 063001 (2012).
- [2] Y. Tsuji *et al.*, Supercond. Sci. Technol. 33, 074001 (2020).
- [3] T. Kawaguchi *et al.*, Appl. Phys. Lett. 97, 042509 (2010), T. Kawaguchi *et al.*, Appl. Phys. Express 4, 083102 (2011).
- [4] K. Kondo *et al.*, Supercond. Sci. Technol. 33, 09LT01 (2020).

Figures

(a) Normalized T_c and (b) J_c of the strip lines as a function of the line width.

Keywords: iron-based superconductor, microfabrication, photon detector



The H content dependence of the anisotropy of NdFeAs(O,H)

*Takafumi Hatano¹, Hiroya Imanaka¹, Hiroto Hibino¹, Hiroshi Ikuta¹

Department of Materials Physics, Nagoya University¹

Among the various iron-based superconductors, $LnFeAs(O_{1-x}F_x)$ and $LnFeAs(O_{1-x}H_x)$ ($Ln = Nd$ and Sm) show the highest superconducting transition temperature T_c of 56 K [1-2]. Both fluorine and hydrogen substitution dope electrons to the system, but the remarkable difference is the solubility limit; it is $x \sim 0.2$ for the former, whereas $x \sim 0.8$ for the latter. Thus, the physical properties can be investigated in a broader range of carrier density with hydrogen doping. Recently we have grown NdFeAs(O_{1-x}H_x) thin films with various x [3] and studied the anisotropy by measuring the resistivity of the films grown on vicinal cut substrates [4]. The anisotropy of the normal state resistivity $\gamma_\rho (= \rho_c/\rho_{ab})$ showed a strong doping dependence and recorded 100–150 at 50 K with the optimally doped films (films whose T_c was higher than 40 K). With increasing the carrier concentration, γ_ρ decreased significantly, but even the most H doped film had a high value of 9. On the other hand, the anisotropy of the upper critical field H_{c2} measured in the superconducting state was much lower [4], although the H content dependence was yet not fully explored.

In the present work, we measured the anisotropy in the superconducting state in a wide range of H content x . The films were grown by the method reported in Ref. [3]. We measured the angle dependence of resistivity under various magnetic fields at temperatures below the zero field T_c and determined the anisotropy ratio of H_{c2} (Γ). Our results indicate that Γ is only weakly dependent on doping and is much lower than γ_ρ . In the standard GL theory, Γ is proportional to the square root of the mass anisotropy. As the mass ratio is also related to γ_ρ , it is notable that the anisotropy parameters are quite different between the superconducting and normal states. We will discuss the possible origin of the large discrepancy between the two anisotropy parameters.

[1] Y. Kamihara *et al.*, J. Am. Chem. Soc. 130, 3296 (2008).

[2] T. Hanna *et al.*, Phys. Rev. B 84, 024521 (2011).

[3] K. Kondo *et al.*, Supercond. Sci. Technol. 33, 09LT01 (2020).

[4] M. Chen *et al.*, Phys. Rev. Mater. 6, 054802 (2022).

PC9-1-INV

ARPES studies of iron-chalcogenide superconductors Fe(Se,S) and Fe(Se,Te)

*Amalia Coldea¹

The University of Oxford¹

Isoelectronic substitution is an ideal tuning parameter to alter electronic states and correlations in iron-based superconductors. As this substitution takes place outside the conducting Fe planes, the electronic behaviour is less affected by the impurity scattering and relevant key electronic parameters can be accessed. In talk I present the experimental progress made in understanding the electronic behaviour of the nematic electronic superconductors, FeSe_{1-x}S_x and FeSe_{1-x}Te_x using angle-resolved photoemission spectroscopy. A direct signature of the nematic electronic state is the in-plane anisotropic distortion of the Fermi surface triggered by orbital ordering effects and electronic interactions that result in multi-band shifts of the different electronic bands. The changes in the electronic structure and their correlations with the superconducting phase diagrams will be discussed.

Keywords: Iron-based superconductors, ARPES

Evidence of interface superconductivity in ultrathin FeSe/STO grown by PLD

*Tomoki Kobayashi¹, Hiroki Ogawa¹, Hiroki Nakagawa¹, Fuyuki Nabeshima¹, Atsutaka Maeda¹

The University of Tokyo, Japan¹

Iron chalcogenide superconductor, FeSe, has attracted much attention because monolayer film on SrTiO₃ (STO) exhibits significant enhancement of superconducting transition temperature (T_c) from 8K to 40---65 K[1,2]. The high T_c in the monolayer FeSe/STO is attributed to the interface effects such as electron doping from STO substrate and the coupling between electrons in FeSe and phonons in STO. Other than in FeSe/STO, such T_c enhancement by the interface effects was reported in different heterostructures, i.e. FeSe/BaTiO₃[3], FeSe/TiO₂[4,5], FeSe/LaFeO₃[6], and FeSe/NdGaO₃[7]. The search for higher T_c and the mechanism of the superconductivity can be explored by fabricating heterostructures of FeSe with different oxide materials. Pulsed laser deposition (PLD) has advantages in fabricating various heterostructures at low cost because different materials can be deposited simply by replacing target materials. However, almost all studies on the T_c enhancement in monolayer FeSe/oxide so far were performed using the molecular beam epitaxy (MBE) technique. We have worked on realizing T_c enhancement in ultrathin films of FeSe/STO using PLD. Previously, we successfully realized T_c enhancement in FeSe/STO with thickness $d \geq 7$ nm[8], which is quantitatively the same as the results in MBE-grown films[9]. To get these results, preparing atomically flat STO substrate is crucial. The high T_c cannot be explained by the strain effect on FeSe established so far[10]. This suggests the realization of T_c enhancement by the interface effects in PLD-grown FeSe/STO. In the early stage, however, for films with $d \leq 5$ nm, superconductivity was not realized possibly because of the sample degradation by the air exposure. This result shows the need for the protection layer to realize superconductivity in thinner films. In this study, we grew ultrathin films of FeSe/STO with capping layers to protect the FeSe films and investigated transport properties under magnetic field. We deposited 10-nm-thick amorphous Si at room temperature as a capping layer. Figure (a) shows the temperature dependence of sheet resistance for capped films with $d = 2-4$ nm. All films showed superconducting transition at low temperatures. onset T_c (T_c^{onset}) of the films are higher than 25 K and much higher than T_c of bulk FeSe ($T_c = 9$ K), suggesting T_c enhancement probably caused by the interface effects. This also indicates the successful role of the protection layer. Figure (b) shows the temperature dependence of the value of R_H/d , where R_H is Hall coefficient, for all films. All films exhibited negative values of R_H/d at low temperatures, which is in good agreement with the results for ultrathin FeSe/STO grown by MBE[9]. This is in contrast to ultrathin FeSe flakes, where R_H has positive values[10]. In addition, positive R_H irrespective of the degree of strain was reported for FeSe thin films grown on substrates other than STO[11]. Thus, these results indicate electron doping from STO substrate. Figure (c) shows the temperature dependence of the resistance under magnetic field H of 0-9 T for the 4-nm-thick film. For $H \perp$ film, T_c^{onset} became lower and the superconducting transition became broader. In contrast, for $H //$ film, superconducting transition was almost unchanged, indicating large anisotropy of critical fields. The estimated c -axis coherence length ξ_c is found to be 0.2 nm which is smaller than c -axis parameter of

FeSe. This suggests that superconductivity is confined at the interface of FeSe/STO.

Figure (a). Temperature dependence of sheet resistance for 2-, 3-, and 4-nm-thick films with capping layers.

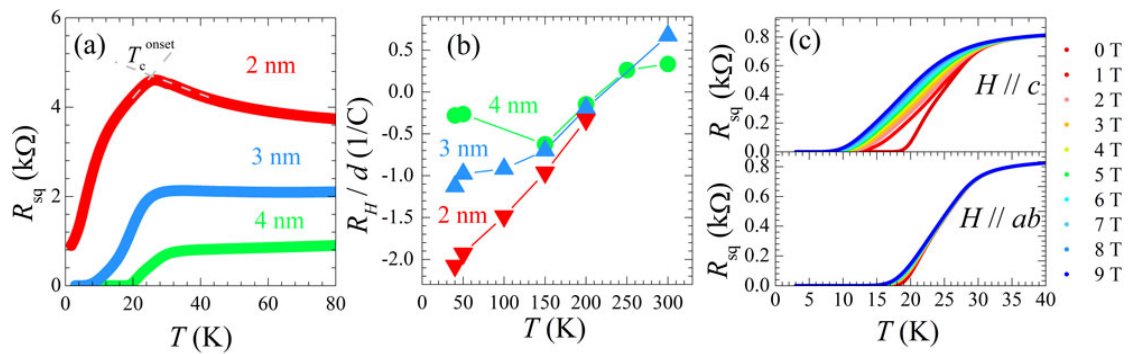
Figure (b). Temperature dependence of R_H/d , for all films.

Figure (c). Temperature dependence of sheet resistance for the 4-nm-thick film perpendicular (top) and parallel (bottom) magnetic field of 0–9 T.

References

- [1]. Q. Y. Wang *et al.*, Chin. Phys. Lett. 29, 037402 (2012).
- [2]. S. He *et al.*, Nat. Mater. 12, 605 (2013).
- [3]. R. Peng *et al.*, Nat Commun. 5, 5044 (2014).
- [4]. H. Ding *et al.*, Phys. Rev. Lett. 117, 067001 (2016).
- [5]. S. N. Rebec *et al.*, Phys. Rev. Lett. 118, 067002 (2017).
- [6]. Y. Song *et al.*, Nat. Commun. 12, 5926 (2021).
- [7]. H. Yang *et al.*, Sci. Bull. 64, 490 (2019).
- [8]. T. Kobayashi *et al.*, Supercond. Sci. Technol. 35, 07LT01 (2022).
- [9]. Q. Wang *et al.*, 2D Mater. 2, 044012 (2015).
- [10]. C. S. Zhu, *et al.*, Phys. Rev. B 104, 024509 (2021).
- [11]. F. Nabeshima *et al.*, Jpn. J. Appl. Phys. 57, 120314 (2018).

Keywords: Iron chalcogenide, Pulsed laser deposition, ultrathin film, Interface superconductivity



PC9-3-INV

Iron-based superconductivity induced by topotactic insertion of light elements (H, O, F) in the LaFeSi intermetallic

*Sophie TENCE¹, Jean-Baptiste VANEY¹, Baptiste VIGNOLLE¹, Etienne GAUDIN¹, Mads F. HANSEN², Marie-Aude MEASSON², Pierre TOULEMONDE², Marc-Henri JULIEN⁴, Fabio BERNARDINI³, Andrés CANO², Alain DEMOURGUES¹

CNRS, Université Bordeaux, ICMCB, UMR 5026, 33600 Pessac, France¹

CNRS, Université Grenoble Alpes, Institut Néel, 38042 Grenoble, France²

Dipartimento Di Fisica, Università Di Cagliari, IT-09042 Monserrato, Italy³

Institut Laue-Langevin, 38000 Grenoble, France⁴

Iron-based superconductors (IBSC) are usually made of building blocks containing iron atoms associated to a pnictogen or chalcogen element (P, As and S, Se, Te respectively)[1]. However, we have recently discovered the first IBSC containing "FeSi" as conductive layer, i.e. the silicide-hydride LaFeSiH ($T_c=10\text{K}$) obtained by solid-gas hydrogenation of LaFeSi [2]. This finding has motivated the research of new IBSC by topotactic intercalation of light elements, like O or F, in intermetallics. However, fluorine and oxygen insertion has remained elusive so far since the strong reactivity of these atypical elements, the most electronegative ones, tends to produce the chemical decomposition of intermetallic compounds.

In this talk, I will present the superconductors we obtained by topochemical synthesis routes and, in particular, I will introduce a new method to intercalate fluorine atoms into intermetallics, using perfluorocarbon reactant with covalent C-F bonds. This novel approach is very efficient to synthesize mixed anion (Si-F) LaFeSiF_x single-crystals in which we observe the coexistence of ionic and metallo-covalent blocks in interaction through inductive effects [3]. Interestingly, we show the emergence of superconductivity across this series, as well as in LaFeSiO_{1-δ}, that thus extends the family of IBSC to novel FeSi-based materials beyond the conventional ferropnictides and chalcogenides [3,4].

References

[1] H. Hosono, K. Tanabe, E. Takayama-Muromachi, H. Kageyama, S. Yamanaka, H. Kumakura, M. Nohara, H. Hiramatsu, and S. Fujitsu, *Sci. Technol. Adv. Mater.* 16, 033503 (2016).

[2] F. Bernardini, G. Garbarino, A. Sulpice, M. Nuñez-Regueiro, E. Gaudin, B. Chevalier, M-A. Méasson, A. Cano, and S. Tencé, *Phys. Rev. B*, 97, 100504(R) (2018).

[3] J-B. Vaney, B. Vignolle, A. Demourgues, E. Gaudin, E. Durand, C. Labrugère, F. Bernardini, A. Cano, S. Tencé, *Nature Comm.* (2022).

[4] M.F. Hansen et al., *npj Quantum Mater.* 7, 86 (2022).

Keywords: Intermetallic, Topochemical synthesis, Iron-based superconductors

Broken time-reversal symmetry in 122-type iron-based superconductors

*Vadim Grinenko¹Tsung-Dao Lee Institute, Shanghai Jiao Tong University, Shanghai, China¹

Any superconducting state breaks spontaneously U(1) gauge symmetry at the superconducting transition temperature (T_c). In some cases, a superconducting state breaks additional symmetries such as rotational lattice symmetry or time-reversal symmetry (Z_2). Usually, multiple symmetries are broken at $T^* \leq T_c$. However, it was predicted theoretically that fluctuations might push T_c below T^* , giving room for a new quantum state of matter, which is different by symmetry from superconducting and normal states [1]. Here, we study the multiband $\text{Ba}_{1-x}\text{K}_x\text{Fe}_2\text{As}_2$ system experimentally. We found that at high K doping levels topological changes of the Fermi surface (Lifshitz transition) trigger a superconducting state that breaks time-reversal symmetry (BTRS) [2,3]. The BTRS superconducting state exists at the narrow doping range $0.7 \leq x \leq 0.85$. More intriguing is that at $x \sim 0.8$, we found a BTRS state at the temperature $T_c^{Z_2} > T_c$ [4]. Evidence for the Z_2 phase transition is given by additional anomalies in the specific heat and ultrasound velocity as well at $T_c^{Z_2}$ we observed an enhancement of the muon spin relaxation rate and appearance of the strong spontaneous Nernst signal (Fig.1). The relation of $T_c^{Z_2}$ to the superconductivity is concluded from similar magnetic field dependencies of T_c and $T_c^{Z_2}$ and by a presence of superconducting fluctuations and a pseudo-gap behaviour above $T_c^{Z_2}$. Based on the theoretical analysis, we proposed that $T_c^{Z_2}$ is associated with a quartic order formed by a correlated state between pairs of Cooper pairs. In this talk, I will also discuss other unusual properties of this state.

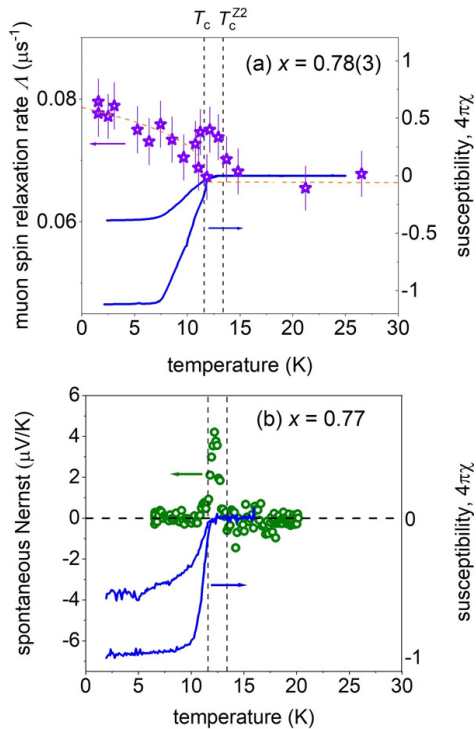


Figure 1: (a) Temperature dependence of the zero-field muon spin relaxation rate (left) shown together with the static magnetic susceptibility measured in $B \parallel ab = 0.5$ mT (right) for the stack of single crystals with $x = 0.78(3)$ [3]. (b) Temperature dependence of the spontaneous Nernst effect measured in zero magnetic field (left) shown together with the static magnetic susceptibility measured in $B \parallel ab = 0.5$ mT (right) for the sample with $x = 0.77$ [4]. The comparison between the μSR data and the spontaneous Nernst signal strongly suggests that the increase of the muon spin relaxation rate above T_c is not an artifact and that the origin of the spontaneous Nernst effect at $T_c^{Z_2}$ is spontaneous magnetic fields.

- [1]. E. Babaev, A. Sudbø, N.W. Ashcroft *Nature* 431, 666–668 (2004). E Babaev *Nuclear Physics B* 686 (3), 397–412 for a review B.V. Svistunov, E.S. Babaev, N.V. Prokof'ev see *Superfluid states of matter* Crc Press (2015).
- [2]. V. Grinenko, P. Materne, R. Sarkar *et al.*, *Phys. Rev. B* 95, 214511 (2017).
- [3]. V. Grinenko, R. Sarkar, K. Kihou, *et al.*, *Nat. Phys.* 16, 789–794 (2020).
- [4]. V. Grinenko, D. Weston, F. Caglieris *et al.*, *Nat. Phys.* 17, 1254–1259 (2021).

Keywords: superconductivity, time reversal symmetry breaking, quartic state, pnictides